FINAL PUBLISHABLE REPORT

Grant Agreement number	16ENG04
Project short name	MyRailS
Project full title	Metrology for smart energy management in electric railway systems

Project start date and duration:	01 September 2017, 41 months	
Coordinator: Domenico Giordano, INRIM Tel: +39 0113 919 826 E-mail: d.giordano@inrim.it Project website address: https://myrails.it/		
Internal Funded Partners: 1 INRIM, Italy 2 CMI, Czech Republic 3 FFII, Spain 4 LNE, France 5 NPL, United Kingdom 6 VSL, Netherlands	External Funded Partners: 7 Comillas, Spain 8 HRI, Italy 9 MM, Spain 10 R.F.I., Italy 11 Railenium, France 12 STRATH, United Kingdom 13 SUN, Italy 14 Trenitalia, Italy	Unfunded Partners: 15 ASTM, Switzerland 16 METAS, Switzerland
RMG: -		

TABLE OF CONTENTS

1 Overview

The project aimed to develop the metrological infrastructure for accurate measurement of energy exchange and reliable system monitoring to enable energy efficient management of the European DC and AC railway and DC subway systems. New facilities for the calibration of the whole energy measurement chains under distorted electrical conditions have provided the metrological infrastructure necessary to improve the reliability of energy billing for railway enterprises. Moreover, the methods developed for the calibration of the energy measurement systems directly on-board the trains will save time and money in the periodic verification of their accuracy. The project also focused on the efficiency assessment of new reversible substations, as well as on the assessment of eco-driving performances. New measurement facilities for the accurate determination of the wasted power in DC railway systems have provided not only means for an energy survey of the railway system but also interesting data that can be deployed towards achieving a more sustainable railway and metro transport system.

2 Need

Considering the overall annual energy consumption of the European railway system, about 36.5 TWh, and the ambitious target of reducing CO_2 railway transport emissions by 50 % by 2030, it is clear that an efficient use of energy in the railway system is required. To this end, accurate and reliable knowledge of the energy absorbed/exchanged between the train and the railway grid that takes harsh on-board measurement conditions into account is essential. In order to establish a single European railway area, the European Commission mandated that energy billings had to be computed on the actual energy consumed by 2019. Consequently, all trains had to be equipped with an energy measurement function (EMF), whose measurement accuracy would be assessed and periodically re-verified in accordance with EN 50463-2. For this, calibration set-ups and procedures which go beyond the well-known procedures developed for pure sinusoidal or continuous regimes were required, to ensure metrological reliability of the EMF under operating conditions.

Efficient use of the infrastructure, as encouraged by the European Union, required new constraints for railway energy supply systems. In this scenario, accurate knowledge of the real-time power quality was a valuable tool to foster the efficiency of the whole railway system by “rewarding” the delivery and absorption of good power quality. Moreover, the saving of energy through eco-driving entailed the application of combined efficient driving strategies to achieve the required running time while minimising energy consumption. The reduction of the absorbed energy had been estimated to be of the order of tens of percent: that was with the same order of magnitude as the uncertainty associated with the on-board energy measurement. There was therefore a need to develop measurement systems able to reduce the on-site absorbed energy uncertainty down to several percent.

3 Objectives

The overall objective of the project was to develop the metrological framework and measurement infrastructure that underpin the adoption of energy efficient technologies in European railway systems. The specific objectives of the project were:

1. To develop a metrological framework for calibration (comprising laboratory and on-board train calibration / measurement set-ups and robust data processing algorithms) to enable high accuracy energy and power quality (PQ) measurements under highly dynamic electrical conditions approaching the uncertainty limits stated in the EN 50463-2:2013-05 with a frequency range from a few hertz up to 5 kHz for AC systems and up to 3 kHz for DC systems. The uncertainty targets for laboratory calibrations are 0.5 % and 0.1 % respectively for AC and DC systems, and 0.4 % for on-board calibration of DC systems. All major European supply systems (25 kV/50 Hz, 15 kV/16.7 Hz, 3 kV/DC, 1.5 kV/DC, 750 V/DC and 600 V/DC) will be considered.
2. To develop a wide-area power quality monitoring architecture. This will include diagnostic studies, system models, numerical simulations, power quality indices definition, measurement system implementation, time-synchronisation, wide-area communication, centralised data collection for quantifying the efficient use of the railway infrastructure and for on-board identification of the PQ events affecting the power exchanged between the supply system and the rolling stock (including high-capacity converter device effects, intermittent sliding-contact arcing and resonance effect).

3. To set up combined measurement-simulation tools to analyse the existing energy-use profiles of DC rolling-stock supplied with traditional unidirectional substations and to quantify the impact of the installation of new reversible substations in terms of energy saving but also in terms of power quality with a target uncertainty of 1 %.
4. To develop accurate measurement systems and procedures for evaluating the energy saving provided by an eco-driving strategy. To reduce the uncertainty of the on-board energy measurement to 1 % to enable assessment of the reliability of an eco-driving forecasting model and to identify and test good practices in on-site estimation of eco-driving benefit.
5. To facilitate the take up of the technology and measurement infrastructure developed in the project by the measurement supply chain (accredited laboratories), standard developing organisations (EN) and end users (train manufacturers, railway companies).

4 Results

Objective 1: Calibration systems for AC and DC Energy Measurement Function

4.1.1 Rationale

The purpose of this objective was to develop a metrological framework comprising laboratory and on-board train calibration / measurement setups and robust data processing algorithms to enable high accuracy energy and power quality (PQ) measurements under highly dynamic electrical conditions approaching the uncertainty limits stated in the EN 50463 2:2013-05 with a frequency range from a few hertz up to 5 kHz for AC systems and up to 3 kHz for DC systems. The uncertainty targets for laboratory calibrations were 0.5 % and 0.1 % for AC and DC systems respectively, and 0.4 % for on board calibration of DC systems. All major European supply systems (25 kV/50 Hz, 15 kV/16.7 Hz, 3 kV/DC, 1.5 kV/DC, 750 V/DC and 600 V/DC) were considered.

4.1.2 AC calibration facilities

Accuracy of power and energy measurements under distorted conditions is an important achievement that the European Commission requires in order to establish a single European railway area. To answer this requirement, two reference calibration setups were developed by FFII and LNE for laboratory calibration of energy measurement systems (EMS) installed in locomotives. The AC calibration facilities developed for AC railway trains are traceable to national standards. Furthermore, VSL developed a setup to calibrate the voltage dependence of AC current transducers operated at medium and high voltages.

Generating high voltage up to 25 kV- 50 Hz and 15 kV-16.7 Hz with harmonics up to 5 kHz, respectively, phase-fired current waveforms going up to 500 A and harmonics up to 5 kHz are the most important achievements of this project. The actual voltage and current waveforms used for the EMF calibration were made available by Trenitalia and ASTM and analysed, in the frequency domain, by Railenium and STRATH. The new calibration facilities developed in this project were also designed for on-board calibrations. They were metrologically characterised to measure distorted waveforms answering thus to the EN 50463-2 requirements. A general setup used to calibrate EMS according to EN 50463-2 standard is composed of:

- power source that should generate high voltages and high currents as required in the EN 50463-2 standard.
- reference measurement system (voltage and current sensors, digitisers and data treatment algorithm to determine the requested quantities).
- measuring the output of the device under test.

LNE completed and validated its calibration setup for the EMS. The capabilities are:

- to generate phantom electrical power consisting of current signal (sinusoidal or 90° phase-fired waveform) up to 500 A rms value and up to 5 kHz harmonic content, at high voltage potential (25 kV, 50 Hz). A 10 MHz signal is used to synchronise voltage and current generation and to trigger the acquisition. This phase-locked loop allows the synchronisation of the calibration system and, thus, the control of the phase displacement between voltage and current for the generation part.

- to compensate the influence of the setup. The attenuation of harmonic amplitudes and phase displacement introduced by the setup components are identified by proper characterisation and appropriate corrections are implemented.

- to measure in a traceable way, the quantities requested by the EN 50463-2 standard with a relative expanded (k = 2) uncertainty of 0.1 % on the active power in sinusoidal conditions and 0.5 % in distorted conditions.

The voltage and current acquisitions are synchronised as illustrated in Figure 1. The sampling frequency is calculated according to the fundamental frequency of the signal to be measured, F, the number of points, N and periods to be recorded, M. One acquisition gets the data corresponding to 5 cycles. The operator starts the acquisition and stops it after the desired number of repetitions.

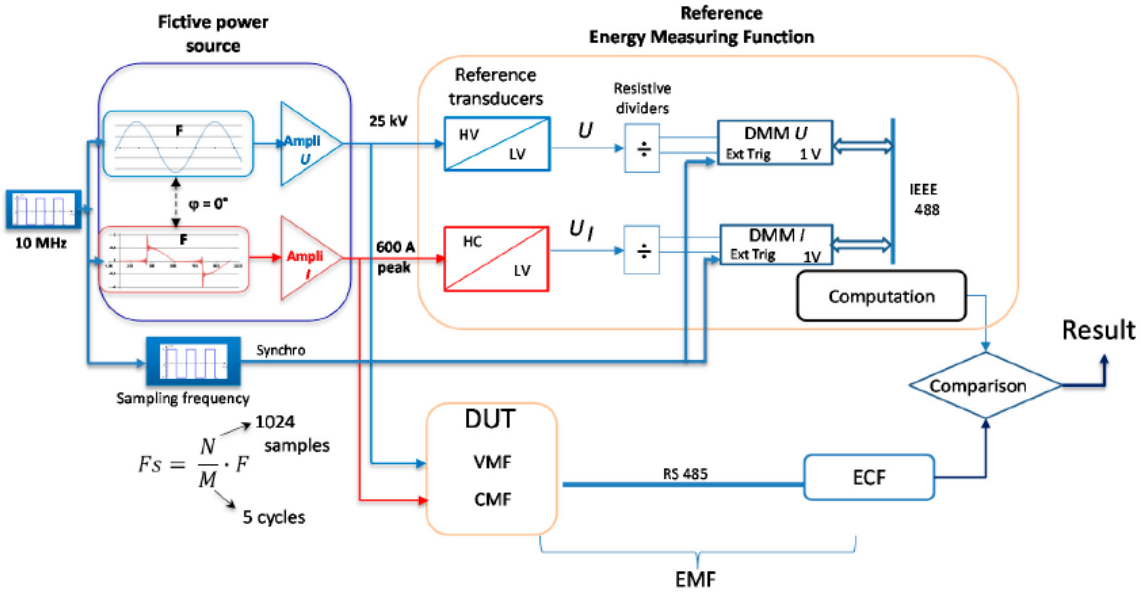

Figure 1. Design principle of EMS calibration setup developed by LNE

FFII, with the contribution of CMI for the uncertainty estimation, completed and validated its calibration setup for the EMS consisting of a phantom power generator composed by two independent but synchronised sources: one source for injecting a sinusoidal current (50 Hz or 16,7 Hz) or a 90° phase-fired waveform up to 500 A rms in a current loop (high voltage insulated cable) and the other source to apply high voltage up to 25 kV, 50 Hz or 15 kV, 16,7 Hz to the current loop.

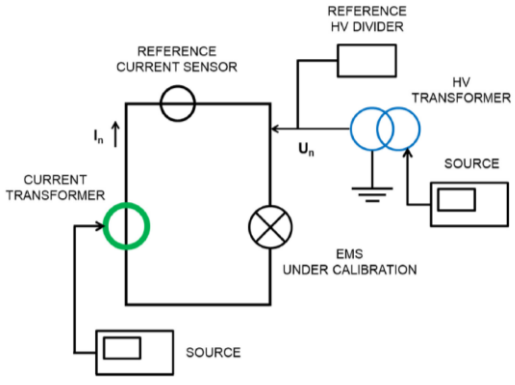

Figure 2. Conceptual Generation setup for 50 Hz and 16,7 Hz developed by FFII.

This phantom generator can work in the two following ways:

- **Voltage with harmonics mode:** to generate phantom electrical power consisting of applying a sinusoidal high voltage up to 25 kV, 50 Hz or 15 kV 16,7 Hz with up to 5 kHz harmonic content to the current loop in which a sinusoidal current up to 500 A is induced.

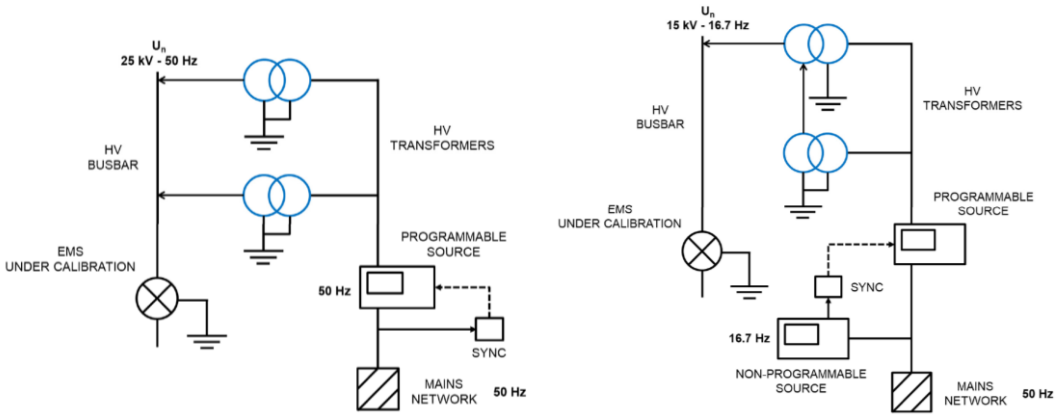

Figure 3. Detail of the high voltage source applied to the current loop (h.v. insultated cable)

- **Current with harmonics mode:** to generate phantom electrical power consisting of injecting a sinusoidal current (50 Hz or 16,7 Hz) or a phase-fired waveform up to 500 A rms value and up to 5 kHz harmonic content in a current loop in which a high voltage is applied up to 25 kV, 50 Hz or 15 kV, 16,7 Hz.

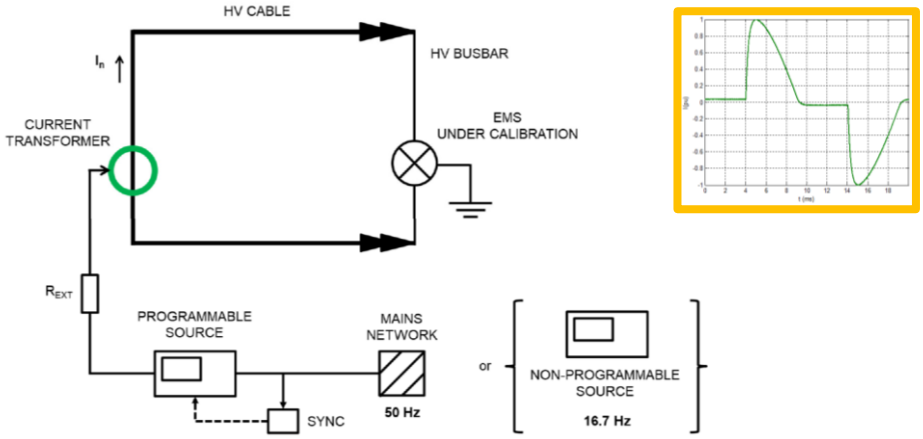

Figure 4. Detail of the high current source injected to the current loop in which the high voltage is applied.

Other features of the system include:

- Both voltage and current sources are synchronised to achieve the required phase displacement between both voltage and current generated signals.
- to compensate the attenuation and phase displacement of harmonic components caused by the magnetic components, a proper characterisation of the calibration setup was performed and corrections in the frequency domain were implemented.
- to measure in a traceable way using an improved high voltage R-C divider, a Fluxgate sensor and two precise Multimeters the quantities requested by the EN 50463-2 standard with a relative expanded (k = 2) uncertainty better than 0.5 % in distorted conditions.

Figure 5. Improved HV divider developed by FFII as the high voltage reference up to 25 kV, from DC to 5 kHz on the basis of previous ENG61 Project 15 k; from DC to 5 kHz 0,1 %.

It is important to outline that the EN 50463-2 standard is based on the AC energy meter for electrical distribution networks. Testing such an energy meter with a distorted current signal of less than 100 A amplitude and harmonics up to 2 kHz is consistent with the reality. However, these amplitudes and frequencies need to be revised for the railway field. Until recently, energy measurement equipment in the railway sector was checked against the requirements of this standard separately for current, and then respectively for voltage and metering, functions (never together) and at levels much lower than their nominal values. Moreover, these verifications and calibrations were done only in dedicated laboratories, never on-board trains due to a missing setup and practice.

Figure 6. Calibration AC facility: for laboratory calibrations (on the left) o for on board calibrations (on the right).

Applying the standard to the railway field characterised by high levels of voltages and currents is not obvious. Problems appear when a distorted high current/voltage need to be generated (rich content of high amplitude harmonics) due to technological challenges. Solutions based on electronic amplifiers (LNE solution) supposes to parallel assembly several current sources, carrying them at high potential and isolating them at 25 kV. This solution has its critical technical, financial and mechanical aspects. The developed fictive power sources rely on the use of magnetic cores that solve the insulation issues. The solution developed by FFII based on current and voltage transformers used to achieve the required high voltage (25 kV 50 Hz and 15 kV 16.6 Hz) and high current (up to 500 A) involved a significant effort in the selection of magnetic components to mitigate saturation effects. Getting adequate electrical insulation was also a challenge. The characterisation in the frequency domain of the magnetic components to perform the corresponding amplitude and phase shift compensation was also an important issue to be resolved. Appropriate compensating algorithms were implemented in the programmable sources used as low voltage and current generators to achieve the required distorted waveforms. The calibration setups and procedures developed in the JRP MyRailS go beyond the state of the art concerning the EMF calibrations.

At VSL, a setup was developed based on a sampling current ratio measurement system to determine the voltage dependence of the ratio error and phase displacement of current transformers (CTs) used at medium voltage (MV) for railway applications (see Figure 7). A grounded shield prevents the reference CT from sensing the high potential applied to the primary current circuit. A novel method was developed to first determine the influence of the applied voltage on the ratio error and phase displacement of the reference circuit. The device under test (DUT) is an MV (or even HV) CT. The overall uncertainty of the calibration system is about 10 ppm (or 0.001 %) for currents up to 5 kA and voltages up to 25 kV, such that the voltage dependent error of the CT under test can be estimated with a typical relative uncertainty of better than 2 % of the error term itself, dependent on the value of the error.

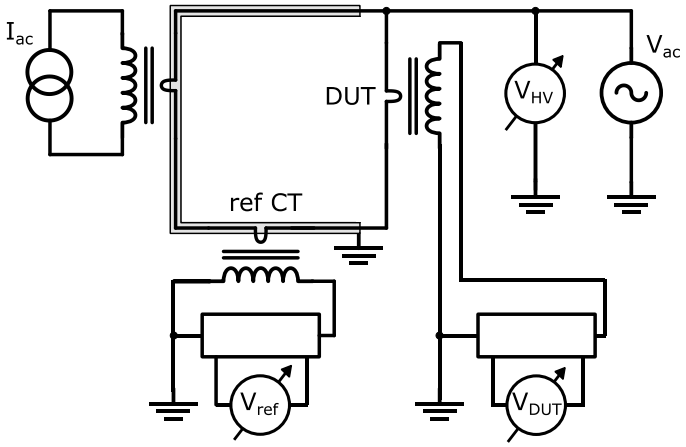

Figure 7. Schematic overview of the VSL setup used to determine the voltage dependence of CTs.

The newly developed reference setup was subsequently used to determine the voltage dependence of a commercial 2500 A class 0,2S MV CT used for railway applications. The size of the voltage dependence was found to be more than two orders of magnitude larger than for the reference circuit, i.e., at 25 kV a ratio error of 3.5 % and phase displacement of 3.5 crad for currents of 25 A, which is the lowest current specified for a 2500 A class 0,2S CT. This is well outside the specified limits of 0.75 % and 0.9 crad set in the IEC 61869-2:2012, which demonstrates that the voltage dependence of MV CTs should be seriously considered when testing them for railway or other applications.

4.1.3 DC calibration facilities

To meet the requirements for the power and energy measurement accuracy under distorted conditions needed to achieve European Commission's goal to establish a single European railway area, INRIM in collaboration with SUN developed a DC power measuring system, METAS developed a method to calibrate the EMC at DC, and VSL developed a system to calibrate DC current transducers under realistic distorted distortions.
INRIM, with the contribution of SUN, developed a new system for the generation of standard DC Power. It is able to generate standard phantom DC power up to 8 MW with the supply voltage ranging from 1 kV to 4 kV and current from 10 A to 2000 A. A schematic drawing of the calibration facility is provided in Figure 8. The system is able to generate both stationary and dynamic electric quantities for 1.5 kV and 3 kV railway systems. Moreover, a superimposed ripple with arbitrary frequency content up to 15 kHz for the voltage and 600 Hz for the current can be generated. The developed reference measuring system allows the determination of the generated power with the uncertainty levels associated with a stationary power summarised in Table I for the 3 kV railway systemunder stationary and dynamic test conditions.

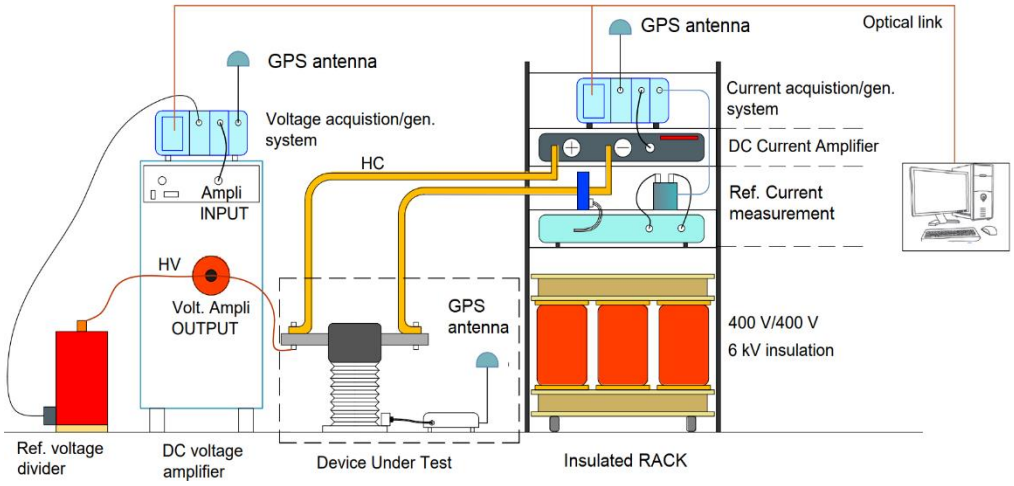

Figure 8. Schematic drawing of the calibration of an EMF for DC application by applying a standard phantom power

Table I – CMC: DC power with voltage ranging from 2.5 kV to 4 kV

Current range	Expanded uncertainty $U(P_{ref})$ for stationary conditions	Expanded uncertainty $U(P_{ref})$ for dynamic conditions[1]
±5 A ÷ ±50 A	150 µW/W	1200 µW/W
±51 A ÷ ±125 A	90 µW/W	900 µW/W
±126 A ÷ ±200 A	110 µW/W	650 µW/W
±200 A ÷ ±375 A	90 µW/W	500 µW/W
±376 A ÷ ±1000 A	110 µW/W	460 µW/W
±1001 A ÷ ±2000 A	90 µW/W	-

[1] The voltage and current test waveforms have to be selected in accordance with the customer

Such a reference system allows the calibration of both the entire measuring chain EMF and the transducer module commonly constituted by a combined voltage-current transducer. The standard generation system, operating in dynamic mode, can reproduce the time behaviour of voltage and current experienced by an EMF during an actual journey of some hours. An example of a dynamic test generated by the reference system is provided in Figure 9. The generation system reproduces the voltage and current signals recorded during a measurement campaign carried out during the project. The fast transient events observed on the red curve were actually experienced in field and are described in the following sub-section.

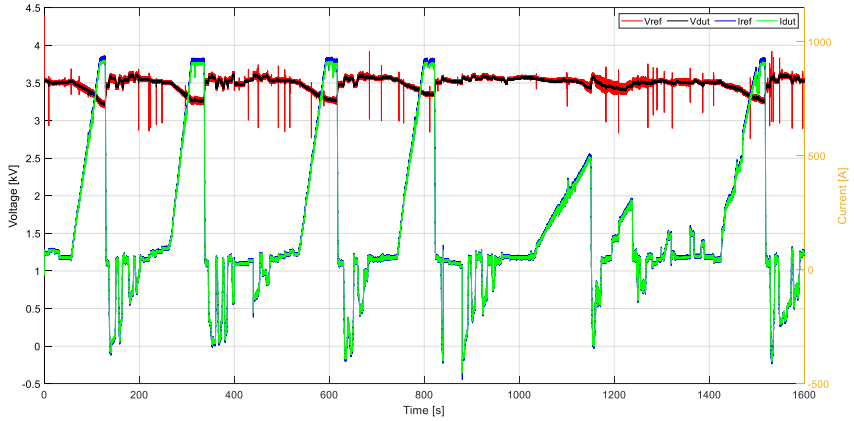

Figure 9. Time behaviour of voltage and current generated by the standard phantom power generator compared with the voltage and current behaviour provided by the device under calibration during a calibration under dynamic conditions.

A measurement setup was realised at VSL to characterise the DC output error of current sensors under realistic operating conditions for railway applications. The total uncertainty of the zero-flux reference sensor was found to be smaller than 10 µΩ/Ω under all distortions. The setup was demonstrated by calibrating a 300 A current shunt with a total uncertainty smaller than 0.05 %, including the intrinsic current dependence, AC distortion, and dynamic current profile that was recorded during a trip between two successive underground train stations from Metro de Madrid.

Finally, METAS has developed a setup for the calibration of the Energy Calculation Function with analog input. The ECF is the module of the EMF that performs the calculation of power and energy starting from the voltage and current information provided by the voltage (VMF) and current transducer (CMF). The uncertainty for the new calibration and measurement capability declared by METAS is of 15 µW/W.

4.1.4 Key output and conclusion

As envisaged by the objective, a metrological framework at the European level was developed and made available to industry to guarantee the reliability of the on-board energy measurements as required by the Commission Regulation (EU) No 1302/2014 of 18 November 2014 concerning a technical specification for interoperability relating to the 'rolling stock — locomotives and passenger rolling stock' subsystem of the rail system in the European Union. A summary of the new calibration capabilities is provided by Table II. The

systems developed can be used to characterise the chains for PQ monitoring. An example is the use of the DC standard generation system to reproduce the quantities at pantograph during an arc event.

Table II New Calibration capabilities

NMI or DI	Quantity	Voltage	Current	Uncertainty	Remarks
LNE	AC power and energy: single phase (f <= 400Hz), active power	1 kV to 30 kV	0,05 A to 500 A	1.10 $^{-3}$ W/VA	Sinusoidal voltage and current. Fundamental frequency 45 Hz to 65 Hz; cosφ: 0 to 1.
				5.10 $^{-3}$ W/VA	Sinusoidal voltage and current with harmonics up to 5 kHz, or 90° phase-fired current waveform. Fundamental frequency 45 Hz to 65 Hz; cosφ =1.
LCOE	AC power and energy: single phase (f <= 400Hz), active power	1 kV to 25 kV	10 A to 500 A	2,2.10 $^{-3}$ W/VA	Sinusoidal voltage with harmonics up to 5 kHz and sinusoidal current. Fundamental frequency 16.7 Hz and 50 Hz; cosφ =0,85 to 1.
				2.10 $^{-3}$ W/VA to 5.10 $^{-3}$ W/VA	Sinusoidal voltage and phase-fired current waveform of 45°, 90° and 135°. Fundamental frequency 16.7 Hz and 50 Hz; cosφ =1.
INRIM	DC power	1 kV to 4 kV	5 A to 2000 A	90 µW/W to 200 mW/W	The system is able to generate the high current with a common mode voltage toward ground of 4 kV. Voltage and current ripple can be generated as quantity of influence up to 15 kHz for the voltage and 600 Hz for the current.
	DC power ratio error	1 kV to 4 kV	5 A to 2000 A	300 µW /W to 450 µW /W	
	DC power under dynamic conditions for voltage and current	2.5 kV to 4 kV	5 A to 2000 A	460 µW /W to 1200 µW /W	
VSL	High AC current: current transformer ratio error and phase displacement	0 to 25 kV	25 A to 2500 A	10 µA/A, 10 µrad	CT under test is operated at specified voltage level and voltage dependent error term is determined.
	DC resistance standards and sources: standards for high current		0 A to 600 A	10 µΩ/Ω	The DC transresistance error of shunts and other current transducers is determined under conditions with AC and dynamic realistic operating distortions in railway systems.

Objective 2: wide-area power quality monitoring architecture

4.1.5 Rationale

The objective was to develop a wide-area power quality monitoring architecture. This includes diagnostic studies, system models, numerical simulations, power quality indices definition, measurement system implementation, time-synchronisation, wide-area communication, centralised data collection for quantifying the efficient use of the railway infrastructure and for on-board identification of the PQ events affecting the power exchanged between the supply system and the rolling stock (including high-capacity converter device effects, intermittent sliding-contact arcing and resonance effect). Three test cases were considered for the on-site measurements: the metro test case, and the railway DC 3 kV and AC 25 kV test cases. For the DC 3kV case, measurements both on-board and in substations were performed.

4.1.6 Facilities for the characterization of the power quality measurement systems

The generation and measurement setup developed by FFII and LNE for the AC and by INRIM for the calibration of EMFs constituted the foundation for the characterization of PQ measurement systems. The harmonic content, which is an influence factor that can affect the measurement of the power and energy, becomes the primary quantities that have to be applied and measured to the device under test which is, in this case, the harmonic content meter. The calibration facility developed for DC, besides voltage and current ripple, is able to reproduce transient events such as the conducted effects triggered by an arc event.

4.1.7 AC power quality monitoring

4.1.7.1 Power quality on-board train

A set of data related to 2x25 KV – 50 Hz acquired at pantograph, made available by ASTM and Trenitalia were analysed by STRATH and NPL. Considering a typical train motion of acceleration – coasting – braking, the voltage THD is always lower than 8 % while the current reaches a THD of 20 %. The 11th harmonic is the most important for both voltage and current during the traction and braking stage while it is almost zero during the coasting stage. The amplitude of the 17th harmonic follows the rms behaviour of the current. It was demonstrated that such harmonics, in particular for the 11th and 17th carried a power of about hundreds of watts.

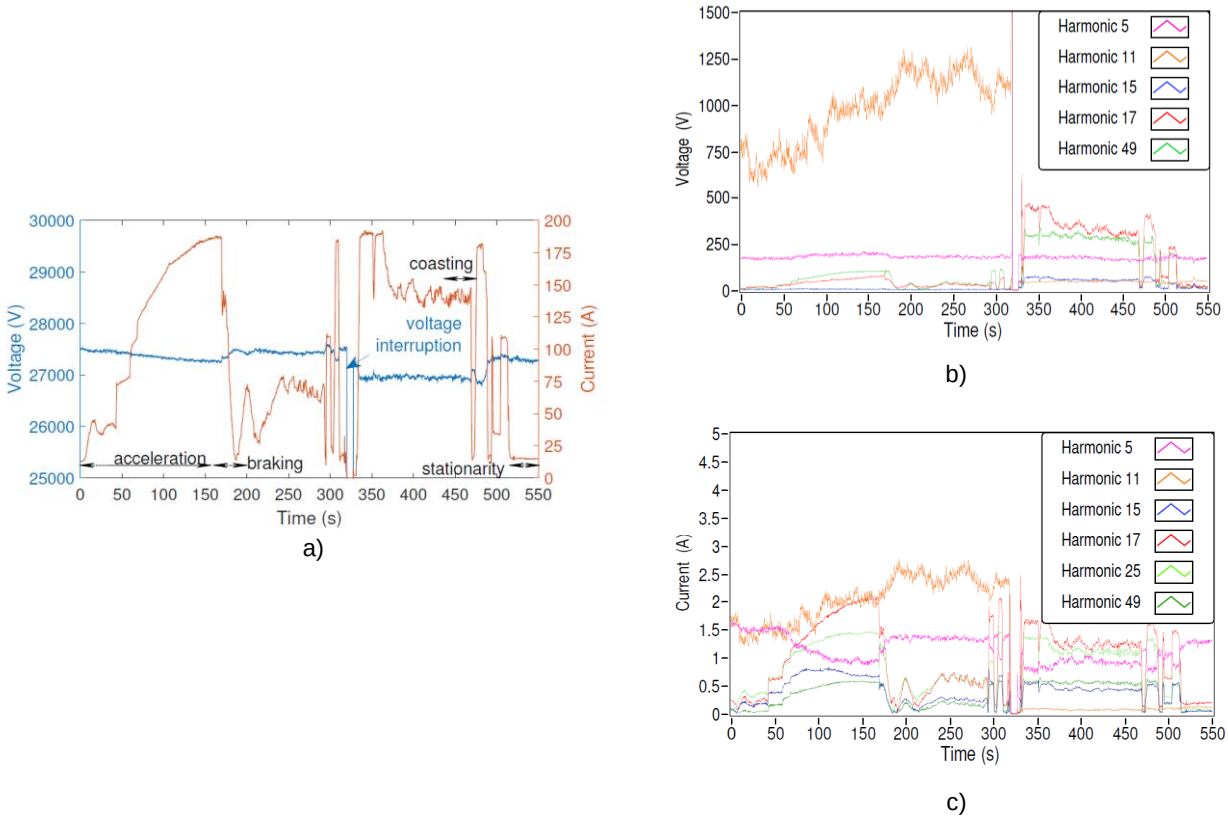

a)

b)

c)

Figure 10. Rms voltage and current behaviour for a real part of a journey a). behaviour of the voltage b) and current c) for the considered time interval

4.1.7.2 The measurement campaign in an AC substation

The quantities of interest for power quality measurements are voltage and current signals. When measuring the 2 x 25 kV system there is a compromise to be made between measurement detail and practicality. Although it would be beneficial to know the voltages and currents in every cell of the section under measurement, the extra cost and effort are not justified by the benefit of the additional information. It was decided to measure the voltage and current at the catenary and the feeder in the TPSS. Due to the high voltage and currents involved in railway operation there is a need for voltage and current transducers that make the quantities measurable with acquisition equipment. Protection-class voltage and current transformers were present in the substation.

It is important not to break the output secondary of the current transformer, therefore a Rogowski coil was used.
The secondary voltage could be measured directly by NPL's digitiser shown in Figure 11 a). This has up to 8 channels, which can be configured as voltage inputs with ranges from 1-400 V or as current channels with built in integrators for Rogowski coils. The voltage measurement has an accuracy of 100 ppm. The sampling rate can be up to 30 kHz and can be internal or external. The samples can be timestamped and synchronised with 1 pulse per second GPS signals. Synchronised measurements are therefore possible between the digitiser on the train and in the substation. Software for the data capture from the digitiser and real time analysis was written by NPL and can be configured to process multiple power quality parameters simultaneously.

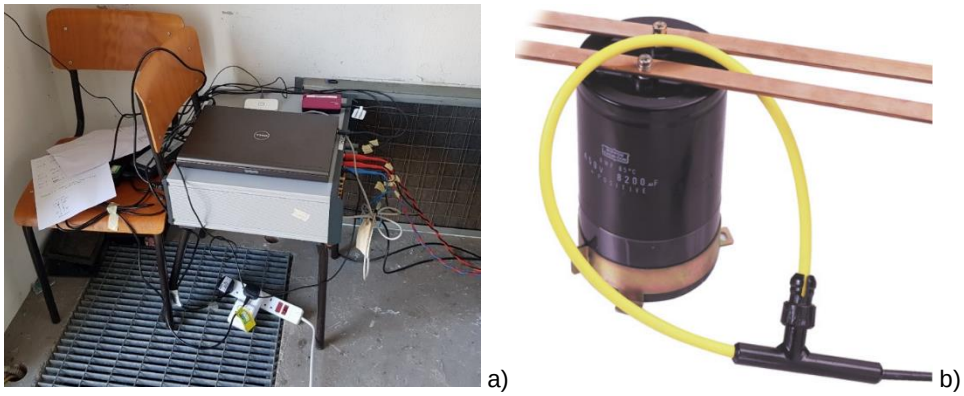
a) b)

Figure 11 – a) NPL digitiser for current and voltage measurements installed in Modena. b) CWTLF current probe for the secondary current measurement

The secondary output current was measured using a PEM flexible Rogowski coil. These have a sensitivity of 200mV/A, 30 A max peak current, 15 mV 1/f noise centered around 0.5 Hz and a phase shift of ~ 0.0757° at 1 kHz. Phase response curves were available and corrected for in the digitiser software. The current probe is shown in Figure 11 b). The Figure 12 provides the block scheme of the infrastructure used for the monitoring and the broadcasting of voltage and current.

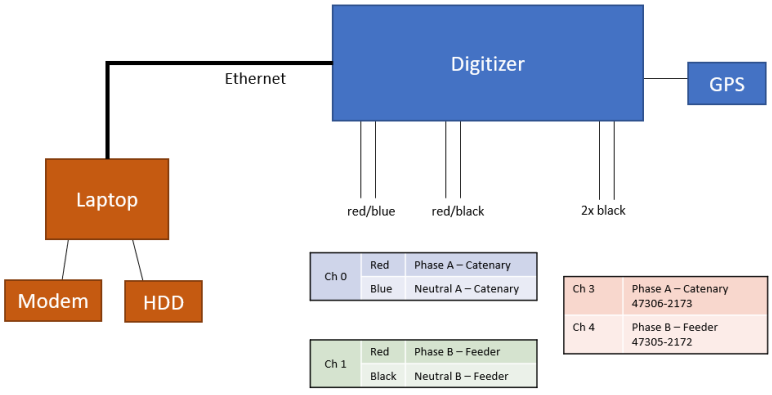

Figure 12. Acquisition System

4.1.7.3 Results of the substation monitoring

The THD for voltage magnitude is shown in Figure 13 for catenary and feeder. There are three sections were the THD is significantly higher than elsewhere. These were three occasions when the line was switched off during night. Therefore, these values do not contain any meaningful information and can be ignored.

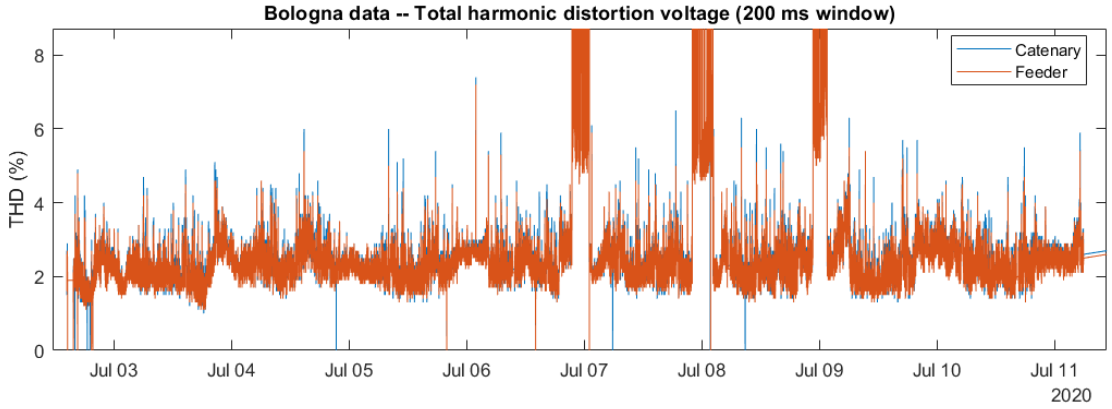

Figure 13. Behaviour of the total harmonic distortion for the catenary and feeder signals

The rest of the data shows THD values for the catenary of between 1 % and 7.4 % with a mean of 2.33 % and for the feeder of between 1.1 % and 7.2 % with a mean of 2.31 %.
For the statistical analysis, the interval of 95 % of values was calculated. This calculation was only performed on the RMS supply voltage of catenary and feeder voltages. The RMS values are based on a 200 ms window. In order to show the difference between using the standard deviation and percentiles, both methods are shown. In order to calculate the values below, only samples above 19 kV were taken into account.

Table III statistical analysis on the catenary and feeder voltage

	Catenary		Feeder	
	Standard deviation	Percentile	Standard deviation	Percentile
95 % interval – lower bound	25.68 kV	25.69 kV	25.70 kV	25.73 kV
95 % interval – upper bound	26.42 kV	26.47 kV	26.42 kV	26.48 kV
% of values that actually lie in this interval	94.4 %	95.0 %	94.6 %	95.0 %

It can be seen that agreement between both approaches is good, and this is consistent with the data concerned following a normal distribution. In general, however, the percentile method should be used if this cannot be safely assumed. Also, it can be seen that for both the catenary and the feeder the values lie well within the safe operating limits for this section and time frame.

4.1.8 DC power quality monitoring architecture

4.1.8.1 The setups for the on-board and in substation monitoring

For the PQ survey in a DC system, four installations were performed: on-board two Italian locomotives for commuter service, the E464 built by Bombardier, on-board the metro-train, S9000 3 CARS, built by Hitachi Rail and operating in Metro de Madrid grid, and finally in a substation close to Forlì (Italy) supplying the Bologna – Rimini route. In the following a detailed description of the setups is provided for each installation.

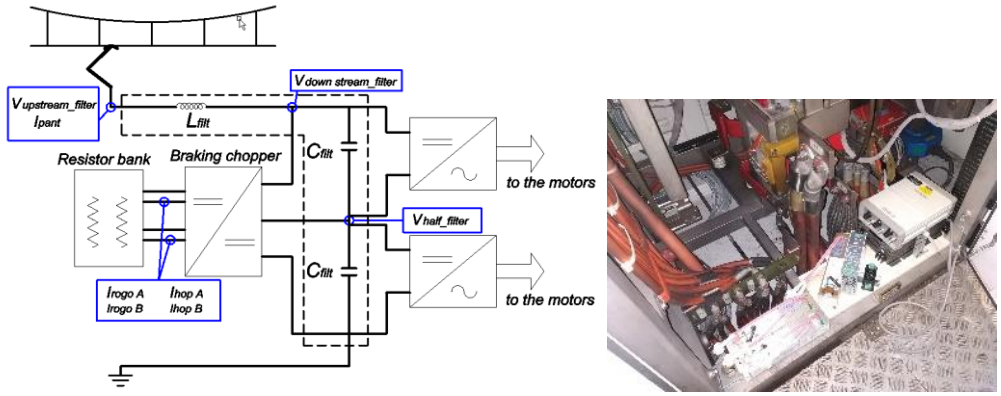

Figure 14. Scheme of the E464 traction architecture a) and s9000 electro-train b) identification and positioning of the monitored quantities

The measurement setup defined for the measurement campaign on-board the DC train consists of an embedded real-time controller from National Instruments (Compact Rio 9034). The controller is equipped with two voltage acquisition modules of four-channels each, having 16-bit resolution (NI 9223), and simultaneous sampling capabilities synchronised to 1PPS incoming from the GPS module (NI9467). One temperature module (NI 9211) was employed to monitor the temperature inside the rheostats room. As shown in Figure 14, 5 the electrical quantities monitored were the voltage and current at pantograph, the voltage after the inductance filter, the voltage in between the two traction inverter modules and the two currents flowing in the braking rheostat module. For the voltage measurement, 40 kV Hultravolt dividers, with a ratio of 1000 and a frequency bandwidth of 1 MHz were used. The current at pantograph was measured by a 2 kA HOP LEM sensor, while the braking currents were measured by both 800 A HOP sensors and by Rogowski coils. The bandwidth of the HOP LEM sensors is 10 kHz while the Rogowski coils have a frequency bandwidth of 30 kHz. A measurement setup similar to that installed on-board trains was installed in the DC 3 kV substation close to Forlì station. The substation is constituted by two parallel connected AC/DC converters, one of which is a mobile converter system placed in a railway carriage, while the other is fixed. The measurement system was placed in the fixed AC/DC converter. The monitored quantities were the current in output (I_p) and input (I_n) of the converter module and the voltage before (V_{upf}) and after (V_{dwf}) the inductance constituting the 100 Hz second order filter. In total four electric quantities were recorded at a frequency of 50 ksample per second thanks to a National Instrument compact RIO system. The data are stored in a 1 Terabyte SD card and periodically replaced.

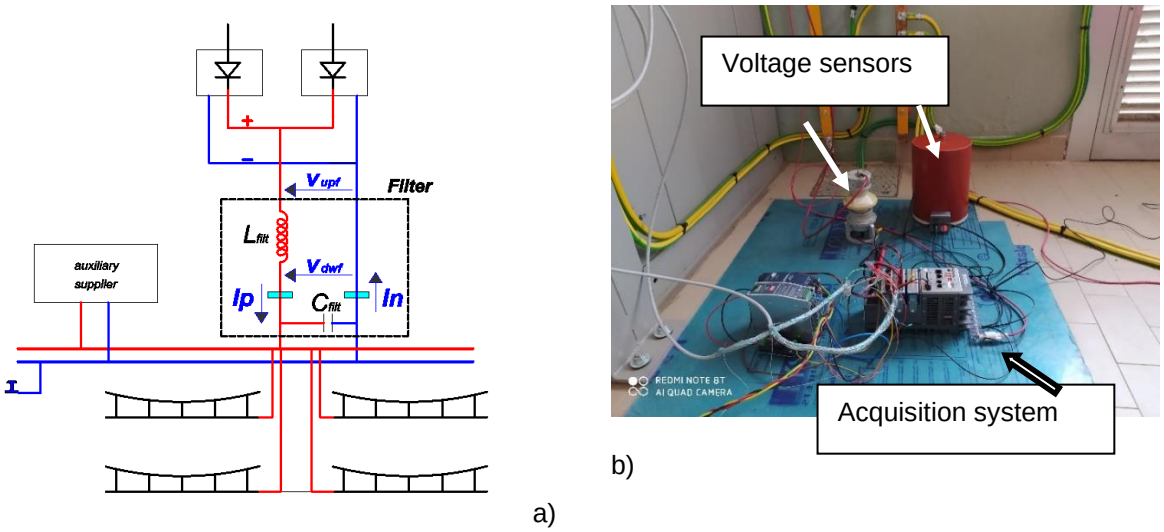

Figure 15. a) scheme of the measurement setup, b) arrangement of the voltage sensors, the supply system and the acquisition system.

4.1.8.2 Measurement campaign results

A statistical analysis was performed over the 122 hours of monitoring of the E464 041 in service on the commuter line in the Piedmont region (Italy). It was found that nearly all values were quite above the nominal value of 3 kV (see Figure 16) and the average value was even greater than U_{max1}. The standard deviation was a few percentages of the mean values (about 120 V). The 95 % percentile was close to 3.8 kV. The first class of histogram reports the occurrence of all the values less or equal to 2500 V. The metro line, on which the rated supply voltage is 1.5 kV, the average value of the supply voltage was higher than 150 V (10 %) of the rated value, the occurrence of which is located in the tail of the histogram of occurrences. Occurrences up to 1.8 kV were detected. The statistical analysis was performed on data recorded continuously for 18 days.

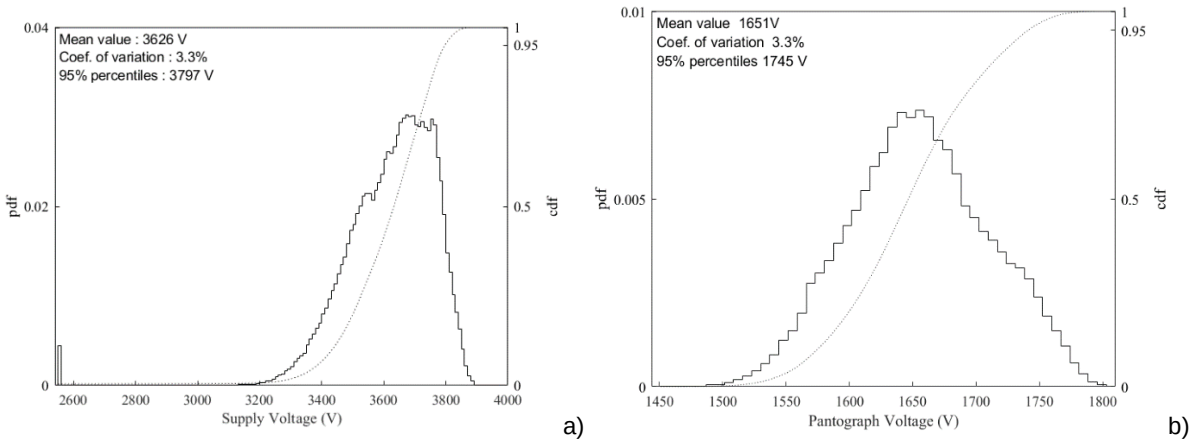

Figure 16. Statistical analysis of supply voltage over all railway routes a) and metro rotes b)

4.1.8.2.1 Statistical analysis on Voltage swell

Figure 17 reports the classification maximum voltage versus duration of all the recorded swell events. The total number of events was 1989 but only 225 of these lasted more than 5 min and maximum voltage reached was greater than U_{max2} in only 23 events. Almost all the events refer to stops at stations or braking events. To understand swell events, it is useful to see the corresponding current shape to distinguish between different situations: the stop at a station is characterised by a nearly constant low current absorption for certain long time while braking is characterised by negative current.

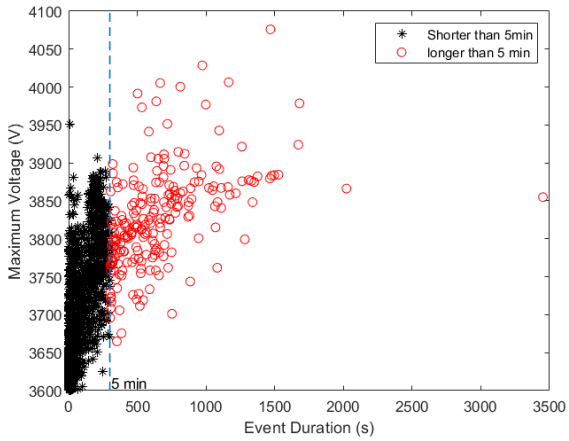

Figure 17. Duration and amplitude of the detected swell events.

4.1.8.3 Voltage oscillatory transient due to rolling stock load insertion

The insertion of burdens in the rolling stock provokes fast voltage transient oscillations. Generally, a large number of such events is detected during a journey. Figure 18 a) gives an example of the frequency of such events during a journey between Bardonecchia and Torino while Figure 18 b) proves that the voltage transient event is triggered by a current step introduced by the insertion of a load in the rolling stock. The events are detected by applying the derivative to the voltage at pantograph. The output signal is compared with a threshold

and every time the signal exceeds the threshold an event is marked; thus the event can be counted. During the journey in question, a total amount of 4277 of such events were detected.

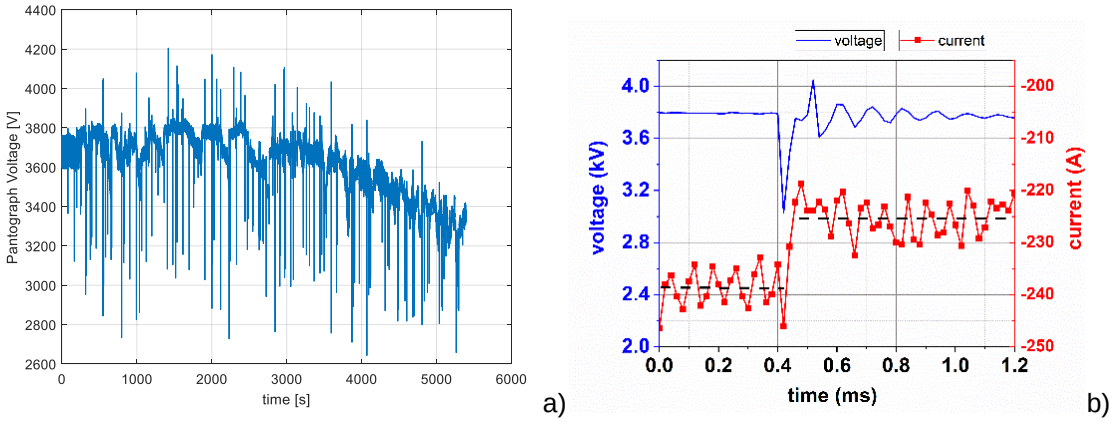

Figure 18. Voltage at pantograph recorded during the Bardonecchia – Torino journey a) zoom of the transient event b)

4.1.8.4 Methodologies for the detection of arc event in DC railway system

An interesting power quality event that characterises the electric railway system is the arc event occurring between the pantograph and the overhead contact line as a consequence of their detachment. Such events can degrade the sliding contact with consequent fault. A simple methodology to detect them can be the basis for the implementation of predictive maintenance of the sliding contact. Two methodologies were developed inside the project. One exploits the voltage and current measurements performed at pantograph for energy billing purposes, the other is based on the analysis of the transient voltage behaviour. The first methodology was submitted for patent and used to look for the arc events in the data recorded in-field by the data-logger developed in the project. A collection of these events were published in an open-access dataset. Figure 19 provides an example of arc events detected in the railway system, during traction and braking stages. The case in the braking stage shows that the increase of the voltage after the filter inductance (V_f) triggers the untimely switching on of the braking rheostat with a consequent increase of the energy wasted. Thanks to the synchronised measurements performed both in substation and on-board a train supplied by the monitored substation, it was possible to observe the same phenomenon (arc event) from the locomotive and the substation. A comparison between the behaviours obtained by the two observation points is provided in Figure 20, where V_p and I_p are the voltage and current measured at the locomotive pantograph while V_b and I_b are the voltage and current measured in the substation.

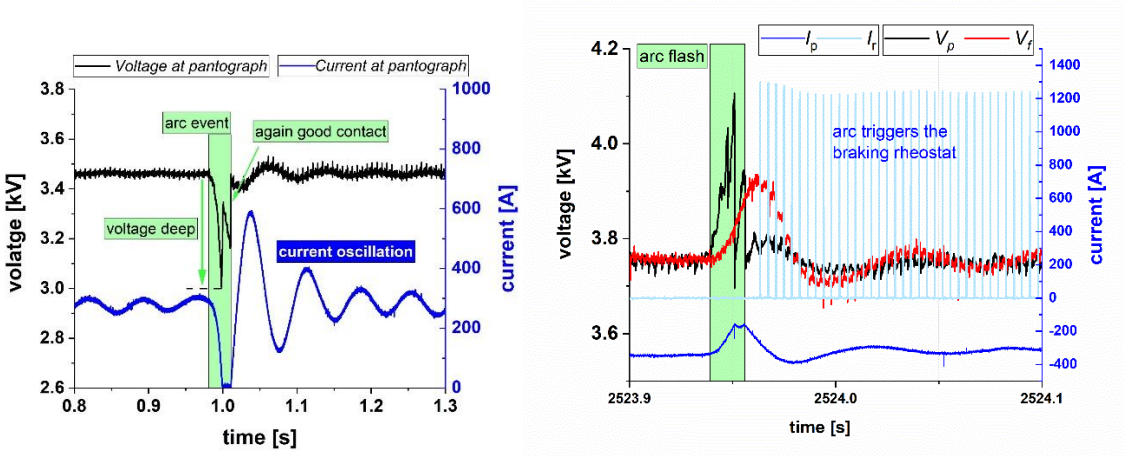

Figure 19. Arc event during a traction stage a) and a braking stage b)

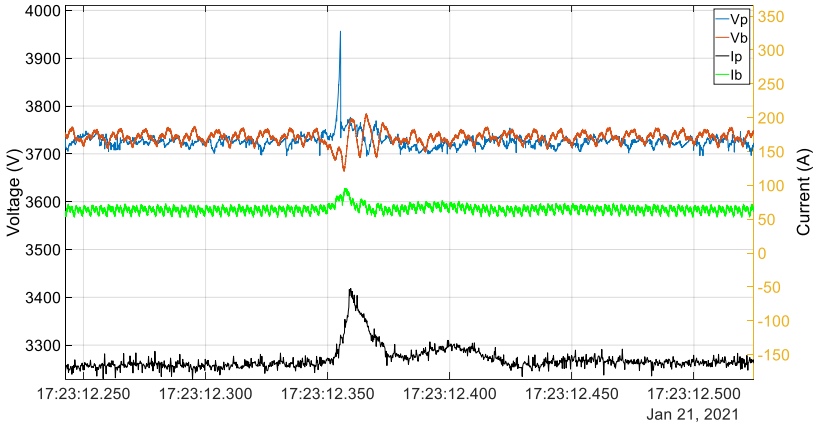

Figure 20 Voltage and current time behaviour recorded on-board and in substation during an arc event

4.1.9 Key output and conclusion

As required by the objective, metrics for the quantification of the power quality of both DC and AC supply systems were established. A deep analysis of the harmonic content on the AC voltage and current at pantograph was performed by Railenium and ASTM. The monitoring of the PQ in the AC substation, performed by NPL with the support of R.F.I., proved the very good quality of the power delivered. A methodology for the determination of the power carried by harmonics was developed by STRATH and METAS and applied to real measurements performed on-board. This activity highlighted the open technical points related to the method implemented in the energy measurement function for energy billing purposes. The activity demonstrated that an algorithm for the energy calculation that extrapolates the phasor at the fundamental frequency provides different results than an algorithm that provides the rms value of the electric quantities.

Concerning DC railway systems, the huge amount of data collected in-field by INRIM, SUN with R.F.I., Trenitalia, MM, and HRI served as the basis for innovative research focused on the identification of PQ events, in particular transient events. Methods for the characterization of DC voltage and current sensors experiencing highly distorted signals were developed by INRIM with the contribution of VSL and CMI. The conducted effects produced by the arc event at pantograph was studied by INRIM, SUN and ASTM combining experimental laboratory work, modelling activity and analysis of data collected in-field. Thanks to this activity, INRIM established a methodology for the detection of such events by exploiting voltage and current measurements performed at pantograph. The methodology has been submitted for patent. Another detection technique was developed by STRATH and METAS. Such techniques provide a valuable tool for diagnostics of the sliding contact between the pantograph and overhead contact line.

Finally, an architecture for the wide-area PQ monitoring implementation was proposed by SUN and INRIM.

Objective 3: Energy dissipated by the braking rheostats and impact of reversible substations

4.1.10 Rationale

To satisfy this objective, characterised measurement setups for on-board applications, algorithms for the analysis of the huge amount of recorded data and a modelling activity for the estimation of the impact of reversible substations (RSS) was carried out.

A method for the accurate determination of the energy wasted by the braking rheostats on-board trains was designed, tested and installed by SUN and INRIM. The selected measurement architecture allowed monitoring over a long period with a sample frequency of 50 kHz. A reliable algorithm for the analysis of these data was developed and tested by SUN.

INRIM with SUN, VSL and CMI defined the model for the measurement of the chopped current flowing in the braking rheostat by identifying and correcting the systematic errors introduced by the measurement setup and the current sensors. The accurate measurement of the chopped current required suitable characterisation procedure of the sensors involved in the on-board measurements. VSL developed a facility for the characterisation, in the time domain, of the sensor by applying a rectangular current up to 600 A. INRIM

characterised the sensors in the frequency domain; that is, by applying a DC signal with superimposed single tone ripple with variable frequency.

The impact of RSS was studied by SUN, INRIM and MM by monitoring the variation in the energy wasted by the braking rheostat of a test train. Two models with increased fidelity levels, developed by STRATH and Railenium, were used to estimate the energy saved on DC railway side and the harmonics generated on the AC upstream grid.

4.1.11 Measurement setup

The measurement setup defined for the measurement campaign on-board the DC train in the Metro de Madrid system consisted of an embedded real-time controller from National Instruments (Compact Rio 9034). The controller was equipped with two voltage acquisition modules of four-channels each, having 16 bit resolution (NI 9223), and simultaneous sampling capabilities synchronised to 1PPS incoming from the GPS module (NI9467). One temperature module (NI 9211) was employed to monitor the temperature inside the rheostats room. A description of the transducers has been provided in the Objective 2 description. Large quantities of data were captured, about 2 Terabytes for the DC railway system. SD cards were periodically replaced to allow new acquired data to be saved and subsequently used to perform dissipated power and energy calculations. Figure 21 provides the location of the measured quantities while Figure 22 shows the actual arrangement in the low voltage and high voltage cabinet.

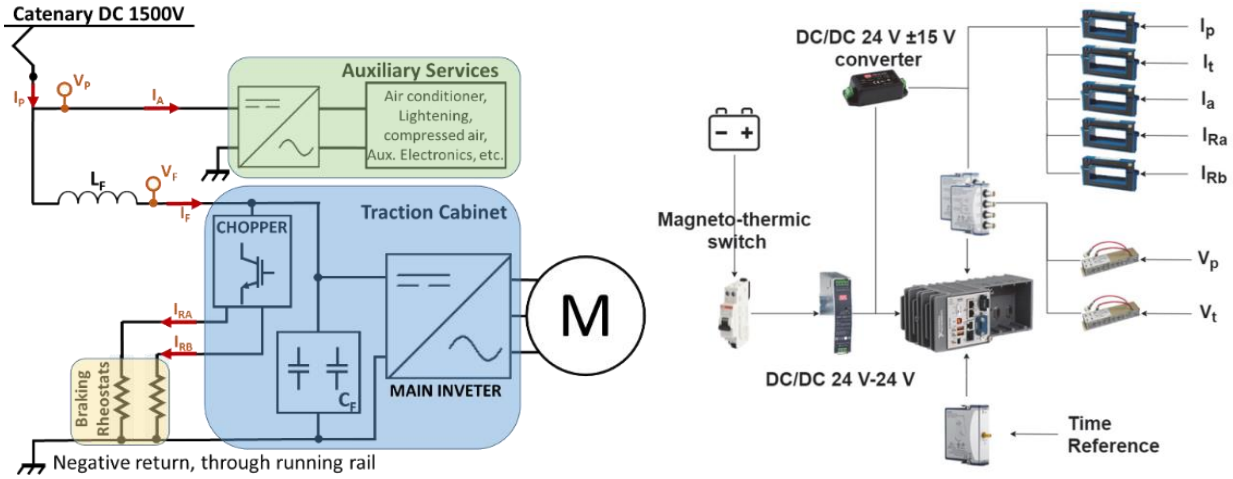

Figure 21. Images of the measurement system installed on board the metro train.

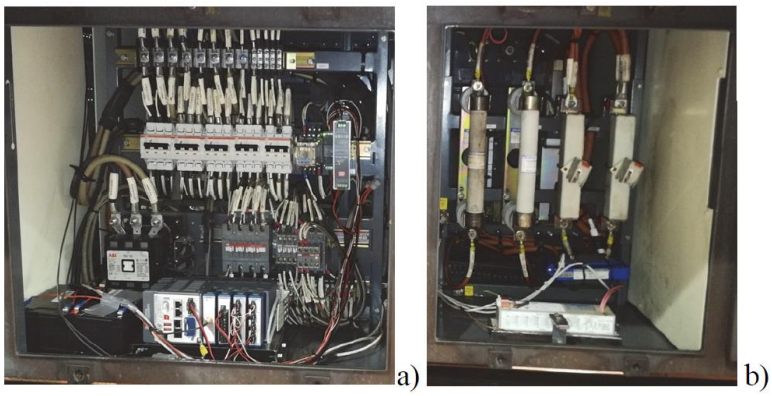

Figure 22. Low voltage cabinet a), and High voltage cabinet b)

4.1.12 Measurement Results

4.1.12.1 Definition of the model of the measurement

To determine the energy dissipated in the braking resistors, two calculation methods were considered. The first method considered the time integral of the instantaneous power calculated from the instantaneous current flowing in each resistor and their respective resistance values. However, because of the large resistance variation (5 %), specified by the producer of the rheostats, this method was found to produce higher uncertainty than the desired target (1 %).

The second method considered the instantaneous current flowing in each resistor and the available measured voltage to calculate the instantaneous power and then the dissipated energy. The sequence of alternating the resistor connections (to two inverters with each pulse) is mathematically implemented by alternately multiplying successive current pulses by the voltage signals ($V_{\text{downstream}} - V_{\text{half-filter}}$) and $V_{\text{half-filter}}$, respectively. To measure the voltage and current signals, voltage transducers are used with voltage ratio k and current transducers with transresistance ratio Rtrans, the latter resulting in ADC readings V_trans^a and V_trans^b. The dissipated energy is then calculated using a discrete form:

$$E = \sum_{i=0}^{N} \left(\left(V_{dsf,i} - V_{hf,i}\right) \cdot \frac{V_{trans,i}^{a}}{R_{trans}^{a}} + V_{hf,i} \cdot \frac{V_{trans,i}^{b}}{R_{trans}^{b}} \right) \cdot \Delta t \qquad (1)$$

However, the proposed power evaluation method was found to introduce two systematic errors. The first is due to the use of the DC voltage at the input of the braking chopper instead of the chopped voltage applied to the rheostat. The second is due to the step response of the transducer affecting the accuracy of the measured current as a result of the large variability experienced by the chopped current (changing from zero to thousands of amperes in short times). To overcome these errors and consequently determine more accurately the wasted energy levels, an accurate model of the electrical braking circuit was developed, and the frequency characterisation of the current transducer was performed to allow appropriate corrective coefficients to be estimated. The proposed measurement model, that provides the correct power dissipated by the rheostat $\bar{P}_{\text{corr}}$ is:

$$\bar{P}_{\text{corr}}(kT) = \left[\frac{1}{T}\int_{k\cdot T}^{(k+1)\cdot T} v_{\text{F}}(t) \cdot i_{R}(t) \cdot dt\right] \cdot K_{\text{DC}}(\delta) \cdot K_{\text{HOP}}(\delta);\ \text{with } k = 0,1,2,\ldots \qquad (2)$$

where k_{DC} and k_{HOP} are the two coefficients that correct the approximated measurement setup and the limited current sensor bandwidth, while $v_{\text{F}}(t) \cdot i_{R}(t)$ are the voltage of the DC link and current flowing in the rheostat respectively. The two correction factors depend on the duty-cycle of the chopped voltage δ_V. As shown in Figure 23, at the increase of the duty-cycle the impact of the correction factor is reduced. Moreover, given an insufficient number of points for a reliable reconstruction of the current pulse with a low duty-cycle, a statistical component in the determination of the coefficient k_{HOP} occurs (see error bars in Figure 23 a).

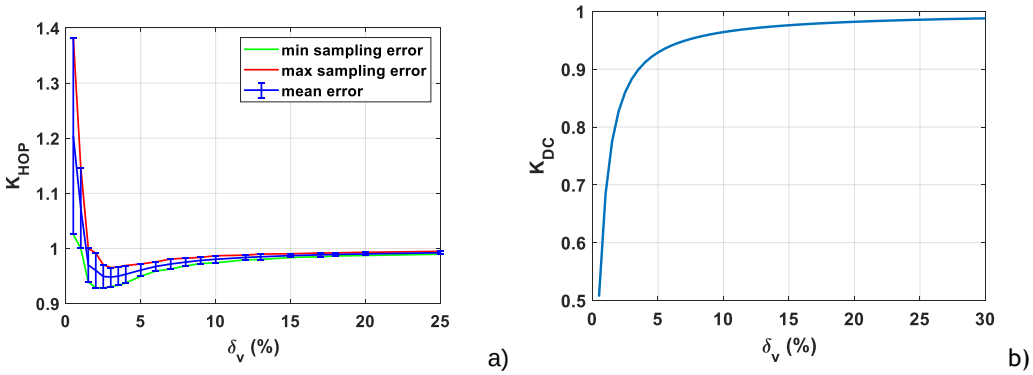

Figure 23 behaviour of $K_{\text{DC}}(\delta)$ a) and $K_{\text{HOP}}(\delta)$ b) versus the voltage duty-cycle

The proposed method was applied to a braking event recorded during the measurement campaign performed at Metro de Madrid. A comparison between the uncorrected and corrected dissipated power was computed, together with the relative deviation between them. The differences ranged between 5 % and 34 % and were more obvious at low levels of dissipated power and normally at low duty-cycles. Because the correction coefficients are also a function of the duty-cycle, the impact of several duty-cycles on the dissipated power is also presented in Table IV. It can be seen that for low duty-cycles the relative deviations are larger, and they decrease with increasing duty-cycle and wasted power.

Table IV Comparison between the power measured *P* and the corrected power for different values of the current duty-cycle.

δ_I	P (kW)	P_{corr} (kW)	Δ (%)	± var (%)
3	13.8	10.3	34	4.3
7.4	54	49	10.2	1.0
10.6	84.2	79	6.6	0.65
16.4	134	129	3.9	0.37

Clearly the accuracy or deviations of the measured power is dependent on the level of the power being measured.

4.1.12.2 Accuracy estimation tool for the dissipated energy

A computational tool for the accuracy estimation associated with the dissipated energy was developed and made available online. The script works in GNU Octave/Matlab and is based on the calculations provided by Equation (1). The script calculates the energy contained in every pulse. The energy of a single braking pulse is calculated by fitting the surrounding noise first to estimate the noise level that affects the accuracy of the calculation, as presented in Figure 24.

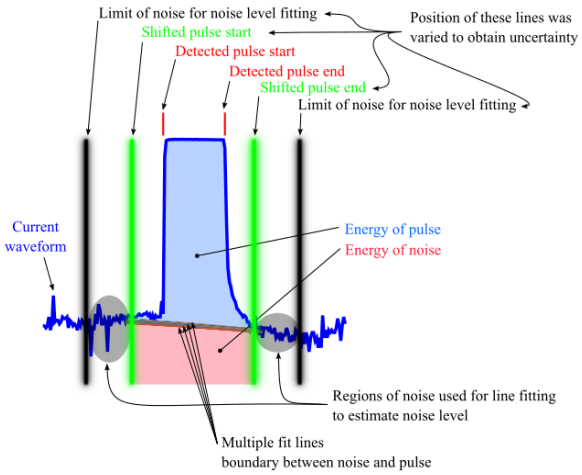

Figure 24 Pulse energy calculation

An arbitrary number of samples between detected pulse start/end, shifted pulse start/end and noise start/end can be specified to allow various noise level estimations and pulse energy calculation, which in turn will affect the uncertainty associated with the energy values of every pulse. The noise level is then subtracted from the pulse to produce the real energy value of every pulse. The energy under each pulse is then integrated to produce the total energy wasted in the braking rheostats. Pulse uncertainty is based on the Monte Carlo method variations of parameters:

- Current offset and gain, independently for both currents acquired by the two sensors.
- Voltage offset and gain, independently for both voltages acquired by the two channels of the digitiser.
- Noise fitting (variation of start/end of noise and pulses).

The uncertainty of all pulses in a group is calculated as a linear sum of pulse uncertainties, which is done for both configurations (see Equation 1). The reason for this is that the correlation is assumed to be 1 (see GUM uncertainty framework, page 21, equation top right). The total uncertainty of all pulses in all groups is calculated as the maximum of all possible permutations of the linear sum of group uncertainties. The accuracy evaluations can be performed for any set of pulses, however there are some issues regarding the method developed which impact on the accuracy of the power calculations and these include: identification problems of pulses based on effective trigger level setting in the software; some braking pulses may be missed at the end of pulse groups, and the nature of the noise to be expected is unknown and how this noise may impact pulse detection requires further clarification.

4.1.12.3 Results

The results of the energy analysis for different train journeys collected during the measurement campaign in the DC railway application are reported in Figure 25. It shows the values of absorbed electrical energy by the train and the total electrical energy generated during braking. The total braking energy is obtained by summing the measured dissipated energy values (wasted energy) with the recovered energy. This last energy is the sum of the energy absorbed by the auxiliary services and that is sent back to the catenary.

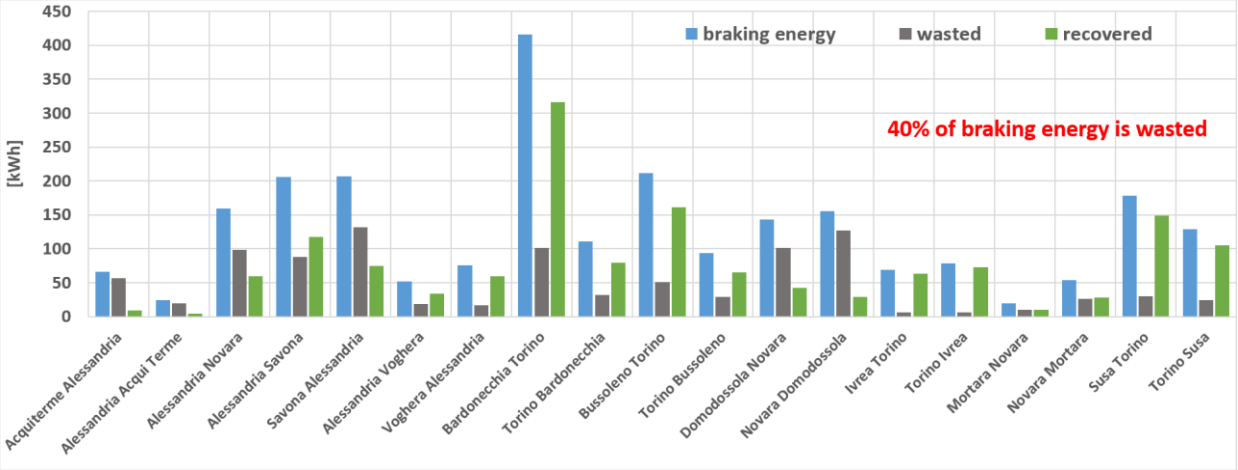

Figure 25 Braking Energy Analysis (rail case study)

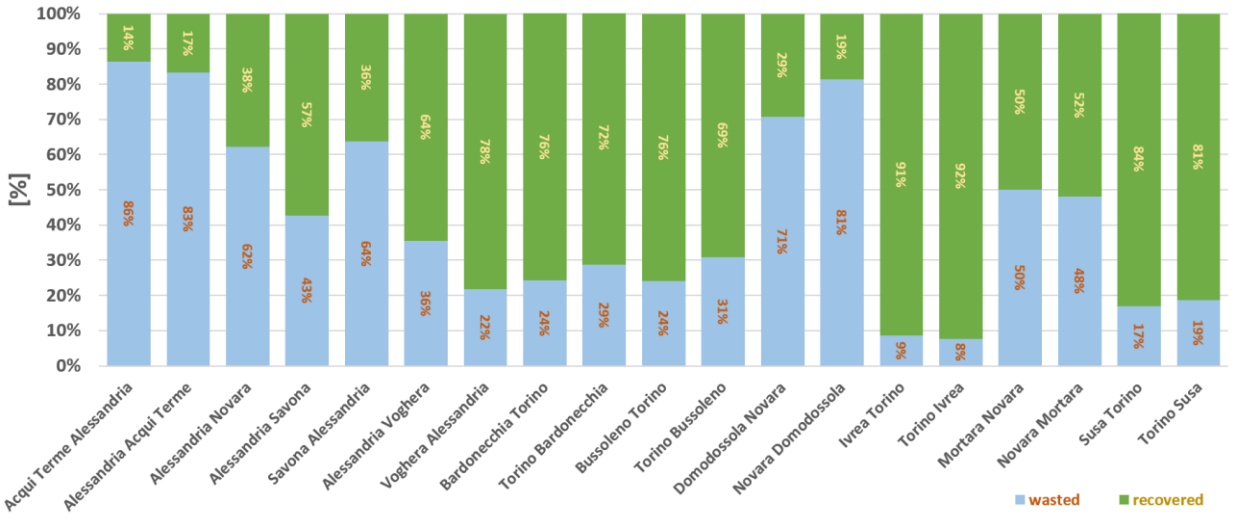

Figure 26 comparison between braking and recovered energy for each monitored journey (rail case study)

As can be seen, a significant amount of regenerative braking energy is dissipated into the braking resistors. In the measurement campaign considered, the total absorbed energy was about 60 MWh; the total amount of energy not recovered was approximately 25 % of the total braking energy, corresponding to around 2.7 MWh. The results of the energy analysis on data collected during the measurement campaign in the DC Metro application are reported in Table V and Table VI. Using acquired current and voltage measurements, the absorbed and regenerated energy of the train during two complete operating days was estimated. Table V, presents the total energy absorbed by the train and the recovered energy resulting from the regenerative braking periods. As presented, significant levels of energy are injected into the overhead contact line, reaching values of around 42 % and 41 % of the total absorbed energy for the respective days.

Table V Comparison between absorbed and recovered energy

Date	*Energy*					
	Absorbed	*Recovered in Power System*		*Net Absorbed*		*Average Absorbed*
		kWh	*%*	*kWh*	*%*	*kWh/route*
14-ott	2.287	970	42%	1.317	58%	79
15-ott	1.870	750	40%	1.120	60%	89

In Table VI, the recovered calculated energy and the dissipated energy in the rheostats, in relation to the total regenerated energy by the train is presented. On both days over 80 % of the braking energy was saved and injected into the contact line, obviously as a consequence of the RSS.

Table VI Comparison between recovered and dissipated energy

Date	**Energy**					
	Generated	*Recovered in Power System*		*Dissipated in Rheostats*		*Average Generated*
		kWh	*%*	*kWh*	*%*	*kWh/route*
14-ott	1092	970	89%	103	9%	37
15-ott	865	750	87%	77	9%	39

4.1.12.4 The impact of RSS

4.1.12.4.1 Measurement determination

The aim is to determine the impact of RSS by considering the energy flow exchanged by the train and the overhead contact line during the braking stages. The considered test case is the line 10 B of Metro de Madrid Network (see Figure 27) on which there is reversible substation at La Moraleja.

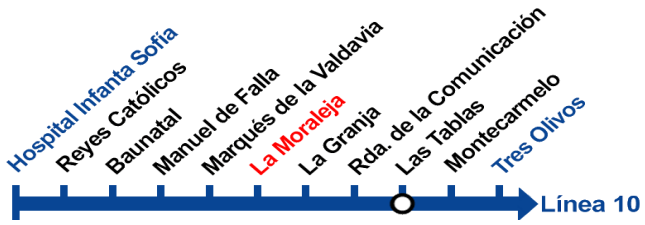

Figure 27 Line 10 B of Metro de Madrid Network

Thanks to the huge amount of data, it was possible to perform a statistical analysis on the energy dissipated by the braking rheostat of the test trains when the reversible was both switched on and switched off. The percentage ratio (DR) between dissipated share, E_d, and total brake energy, E_{br}, can be derived as:

$$DR = 100 \cdot (E_d/E_{br}); \quad where\ E_{br} = -E_t\ with\ \ E_t < 0$$

where E_t is the traction energy. Comparing the results obtained in conventional conditions with those in reversible conditions, one can observe a reduction of the dissipated share on the total that can be appreciated on both mean values (decrease of 2 %) and 95 percentiles (decrease of 4.3 %). Deeper analyses on the acquired data can be implemented taking into account the turnout of the subway line. In particular, using the time table of Metro de Madrid, it was possible to separate the data collected when a high number of trains were in service from that collected when a lower number of trains were in service. It was observed that the number of trains directly impacts on line receptivity. Figure 28 and Figure 29 provide the quantity DR evaluated respectively with n=13 and n=3. A higher number of trains (n=13) means a higher probability to reinject the braking energy on the line. In low receptivity, the effect of the reversible substation is more evident, because of the low number of trains (n=3): during the braking there are less chances of having another train accelerating at the same time. With high receptivity (Figure 29 a and b) the difference between conventional and reversible is about 2 % for the mean value and 3.6 % for the 95 percentile. With low receptivity (Figure 28 and b) the difference between conventional and reversible is more remarkable, reaching about 5.3 % for the mean value and 13.9 % for the 95 percentile.

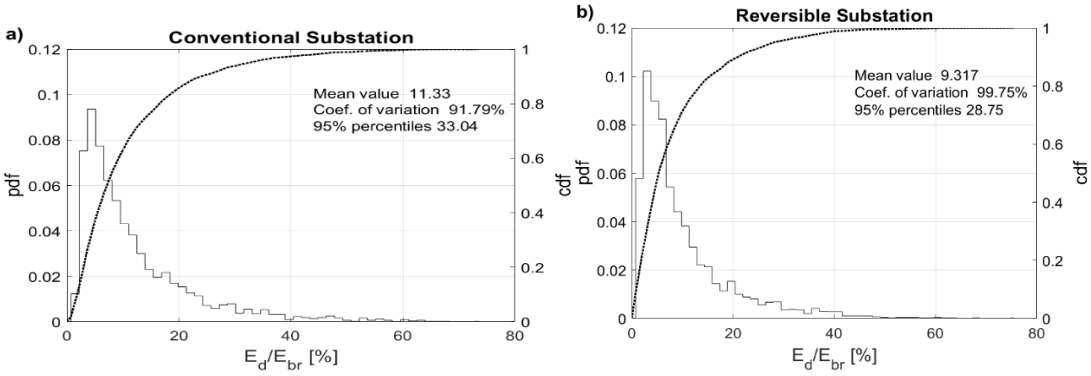

Figure 28 Dissipated energy percentage statistic.

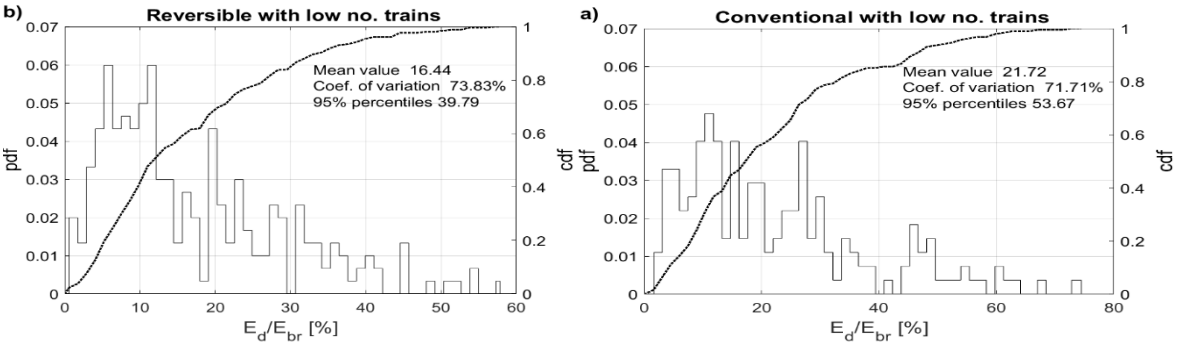

Figure 29 Dissipated energy percentage statistics in case of low receptivity.

4.1.12.4.2 Modelling activity

Two models to reflect the role of an RSS under high and low fidelities, focusing on the converter and TPSS-level simulation, were developed by STRATH and Railenium respectively. A particular RSS topology consisting of a 12-pulse diode rectifier and an antiparallel active neutral point clamped voltage source inverter (VSI) is replicated in a high-fidelity model where the VSI is controlled to maintain a constant DC voltage in the braking mode. To reduce computation burden, a low-fidelity model simplifies the rectifier into a diode in series with a controlled voltage source (CVS) that reflects its nonlinear output characteristics, and connects a DC voltage source in parallel with the CVS branch, permitting the delivery of braking power to the RSS under the constant DC voltage control. The two models were tested based on a simplified 1.5 kV TPSS. Only one train operating is considered.

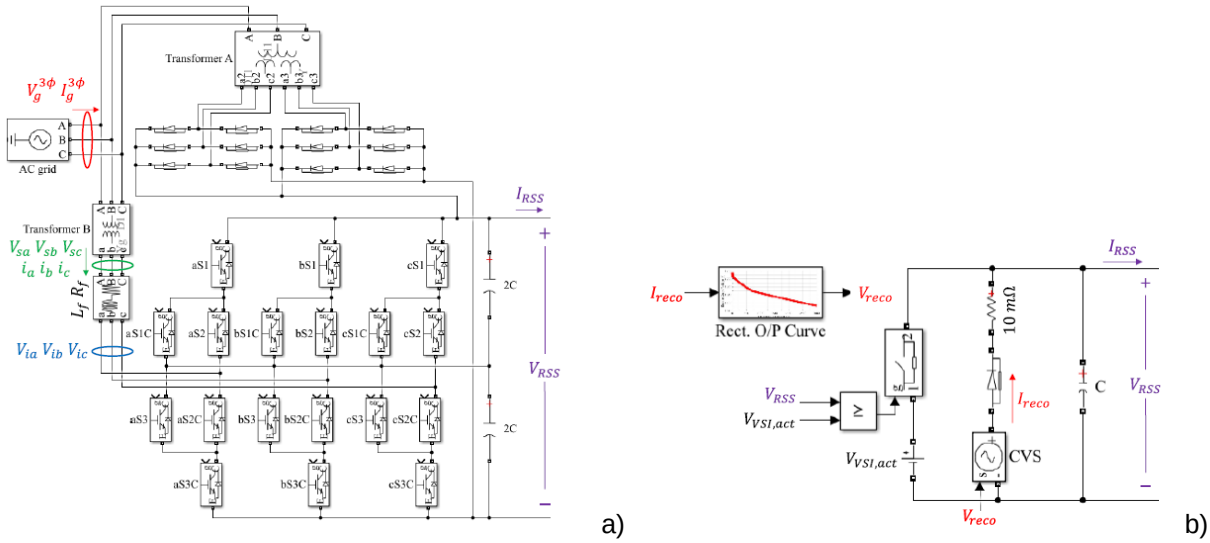

Figure 30. the RSS high fidelity model a) and low-fidelity one b)

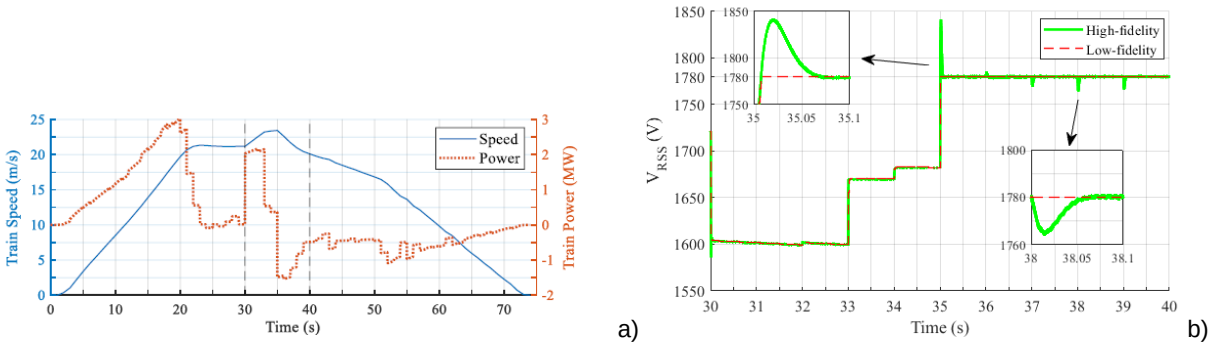

Figure 31 simulated Speed and absorbed/generated power of the train a) comparison between the computed V_{RSS} provided by the high and low fidelity model b)

The high- and low-fidelity models were developed using Matlab/Simulink, and were both simulated at a time step of 5 μs based on the presumed train speed profile during 30s – 40s. The computation time used by the high-fidelity model was reduced by about 80 % in the low-fidelity model. In addition, the two models showed good consistency in the simulation of the power exchange and DC voltage transients at the RSS for the majority of the time. Compared to the low-fidelity model, the high-fidelity simulation was able to reflect transient changes of the DC voltage at the RSS under the constant DC voltage control method, especially at the start of the braking mode and when the recovered braking power changes stepwise. Furthermore, the high-fidelity simulation permitted evaluation of the THD of the AC current fed by the RSS, which was around 3.82 % in a particular 0.02-s cycle in this study.

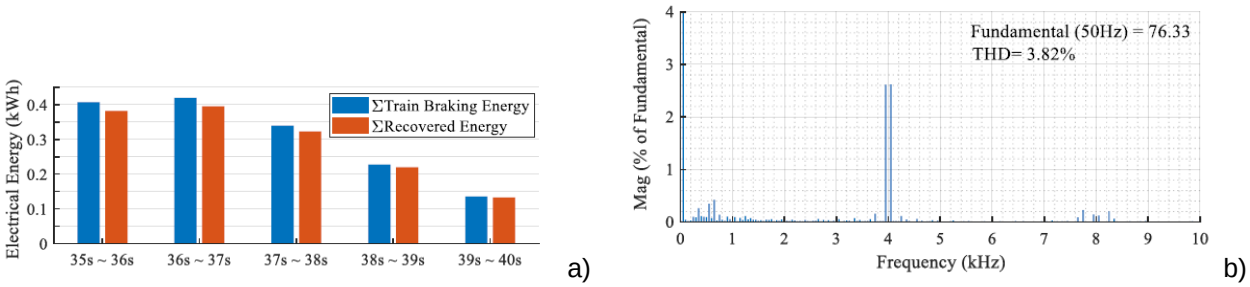

Figure 32 a) The frequency spectrum (% of 50Hz component) of the current along phase A in a particular cycle over 35.1s – 35.12s in braking mode.

The current THD mainly comes from the components around 4 kHz, i.e. twice the switching frequency of the IGBTs within the VSI.

4.1.13 Key output and conclusion

The project objective was met. The activities for the determination of the energy wasted by the braking rheostats in DC railway systems were very innovative in the railway context and provided information that will be useful to future designs for a more sustainable railway system. The metrological skills provided by INRIM, VSL, CMI, NPL and SUN allowed the development of methodologies for the characterisation of current sensors to measure square waveforms, measurement models for the accurate determination of the power and energy absorbed by braking rheostats, and a measurement architecture for continuous monitoring of electrical quantities on-board trains. These activities were possible thanks to the knowledge provided by Trenitalia, R.F.I.; MM and HRI on the monitored traction systems and R.F.I. on the infrastructure features. A modelling activity devoted to the estimation of the RSS impact on both AC and DC supply side was performed by the collaboration between STRATH and Railenium.

Objective 4: Accurate measurement of energy saving provided by eco-driving

4.1.14 Rationale

As required by objective 4, methodologies for the accurate determination of the energy saving provided by eco-driving strategies were developed and applied to metro and railway test cases. To this end, a measurement set-up for monitoring electric quantities was developed, such as algorithms for the determination of energy flux on-board trains. Eco-driving strategies were determined for both Automatic Train Operation (ATO - the on-board automatic driving equipment) and manual application and applied to real test cases. The metrological contribution in the uncertainty determination of simulated on-board train energy fluxes and the run-time computation has provided the knowledge to satisfy the need for accurate determination of the saved energy.

4.1.15 Eco-driving in Metro de Madrid

Activities focused on simulations to assess the eco-driving benefit. The aim was to accurately estimate the energy savings and the associated uncertainty provided by use of an optimum driving strategy based on measurement results. Taking into account the timetable, the rolling stock and railway line characteristics, and the trip time margin, a speed profile for a journey which minimises energy consumption can be found by means of optimisation algorithms. Initially the test cases were identified. In Metro de Madrid, the test cases selected were 4 interstations on Line 10-B, between Marqués de Valdavia y Hospital Infanta Sofía. The 4 interstations are the following:

Table VII Metro line section tested

Interstation	
Origin	Destination
M. Valdavia	M. Falla
M. Falla	Baunatal
Baunatal	R. Catolicos
R. Catolicos	H. Infanta Sofía

For each interstation the test cases were characterised using information on the infrastructure, the train and the ATO. With this information the 4 interstations were modelled and simulated supposing initially a reference driving style (with the ATO), calculating the expected energy consumption and the running time. Then, an optimisation algorithm was executed to design the eco-driving, taking into account the specific characteristics of the ATO equipment on-board these trains running on line 10-B. The results of the optimisation are the calculation of the following ATO driving parameters.

Table VIII Optimal ATO driving parameters

Interstation		ATO driving parameters			
Origin	Destination	Braking deceleration (m/s2)	Coasting speed (km/h)	Remotoring speed (km/h)	Remotoring speed (km/h)
M. Valdavia	M. Falla	0,6	80	30	30
M. Falla	Baunatal	0,6	50	10	10
Baunatal	R. Catolicos	0,6	55	10	10
R. Catolicos	H. Infanta Sofía	0,6	60	10	10

- Braking deceleration parameter is used when trains reduce their speed to stop at stations.
- Coasting speed parameter is used to turn off the traction effort once the train speed reaches this value.
- Remotoring speed parameter is used to turn on the traction effort again, once the train speed has reduced this value compared to the coasting speed parameter.

The associated energy consumption and running times of the designed eco-driving are obtained by simulating these 4 interstations with the selected driving commands of the ATO. The following table shows the simulated energy consumption and running times of the reference driving and the eco-driving for each interstation, and

the expected energy savings in percentage. The selected test cases were tested as well on Line 10-B in Metro de Madrid with a train running along these 4 interstations, and measurements were recorded on-board the train.

Table IX Simulated energy consumption and running times

Interstation		Reference		Ecodriving		
Origin	Destination	Running time (s)	Energy consumption (kWh)	Running time (s)	Energy consumption (kWh)	Energy Savings (%)
M. Valdavia	M. Falla	106,45	19,64	114,15	16,66	15,18%
M. Falla	Baunatal	72,90	8,94	79,75	4,24	52,63%
Baunatal	R. Catolicos	83,10	8,94	89,75	5,09	43,08%
R. Catolicos	H. Infanta Sofía	117,35	10,24	122,25	6,21	39,36%

4.1.15.1 Experimental energy analysis

For the following analysis, we refer to the energy measurement system that was already installed on-board the train. It was modified in its basic behaviour to be able to measure and record the total traction current consumed by the motors and the voltage at pantograph every 250 ms. Traction electric power is obtained by multiplying these two magnitudes, and then the total energy consumed by the motors in each interstation is calculated by adding the energy consumed every 250 ms along the journey.

The following table shows the measured energy consumption and running times of the reference driving and the eco-driving for each interstation, and the measured energy savings in percentage.

Table X Measured energy consumption and running times

Interstation		Reference		Ecodriving		
Origin	Destination	Running time (s)	Energy consumption (kWh)	Running time (s)	Energy consumption (kWh)	Energy Savings (%)
M. Valdavia	M. Falla	106,45	19,63	116,50	16,66	15,12%
M. Falla	Baunatal	72,90	9,19	80,60	4,34	52,78%
Baunatal	R. Catolicos	83,10	9,12	90,50	5,12	43,80%
R. Catolicos	H. Infanta Sofía	117,35	10,48	114,10	6,33	39,59%

4.1.15.2 Comparison between measurement and simulation

The following table shows measured and simulated energy savings and the running time differences due to the application of the designed eco-driving, and the associated errors.

As shown in the previous table, the expected energy savings provided by the designed eco-driving were accurately estimated by the simulation model. At each interstation the percentage of energy savings measured are very close to the expected ones. In conclusion, the proposed method for the estimation of energy savings based on simulation was demonstrated to be an accurate procedure.

Table XI Measured energy consumption and running times

Interstation		Running time differences			Energy savings		
Origin	Destination	Measurement (%)	Simulation (s)	Error (%)	Measurement (%)	Simulation (s)	**Error (%)**
M. Valdavia	M. Falla	8,27%	7,23%	1,04%	15,12%	15,18%	**-0,06%**
M. Falla	Baunatal	8,48%	9,40%	-0,92%	52,78%	52,63%	**0,15%**
Baunatal	R. Catolicos	7,48%	8,00%	-0,52%	43,80%	43,08%	**0,72%**
R. Catolicos	H. Infanta Sofía	6,84%	4,18%	2,66%	39,59%	39,36%	**0,23%**

4.1.16 Eco-driving along the Bologna-Rimini line

The eco-driving activity for the railway test case was applied along the DC 3 kV line between Bologna and Rimini. The test train was constituted by the locomotive E464-354 and conventional rolling stocks. The measurements were performed during regular commercial service, which limited the free application of the eco-driving strategy. The weight of the train varied between 316 *t* and 361 *t* due to different train compositions. The interstations analysed in Bologna-Rimini line were:

- Rimini - Cesena
- Cesena - Castel Bolognese
- Castel Bolognese – Castel San Pietro
- Castel San Pietro – Bologna

4.1.16.1 Experimental Energy Analysis

The on-board electrical quantities were recorded by the setup described in the section above concerning objective 2. The train speed and traction effort were provided by the tele-diagnostic system with a sample rate of one hertz. The electrical quantities monitored were: I_p (pantograph current), I_{aux} (auxiliary systems current), I_r (rheostat current), V_f (voltage after the filter), V_p (pantograph voltage). The raw data were recorded with a sample frequency of 50 kHz. Since the energy determination does not require a so high a sample frequency, the data were processed in order to provide a sample every 0.01 s or 0.1s. The analysis was focused on Rimini-Cesena and Castel San Pietro-Bologna interstations. As an example, the behaviour of the computed vs measured speed profiles and traction efforts for the reference and eco-driving cases associated with the Rimini-Cesena interstation is provided in Figure 33 a) and b) respectively.

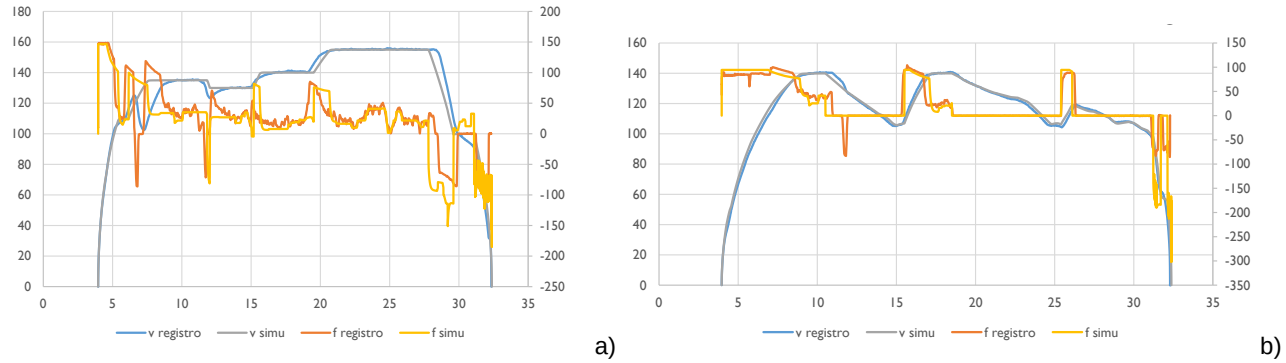

Figure 33 Rimini-Cesena. Behaviour of measured and simulated speed and traction effort for the reference a) and eco-driving b) case

4.1.16.2 Comparison between measurement and simulation in terms of energy savings

In the following tables the simulations are compared with measurements and the energy savings are evaluated:

Table XII Simulated energy and running time

Simulation

		Reference		eco-driving		differences	
		running time	energy	running time	energy	time difference	energy savings
Rimini	**Cesena**	865	308,365	980	247,425	13,3%	19,8%
Castel San Pietro	**Bologna**	846	213,994	883	173,54	4,4%	18,9%

Table XIII Measured energy and running time

Measurements

		Reference		eco-driving		differences	
		running time	energy	running time	energy	time difference	energy savings
Rimini	**Cesena**	873	311,35	992	260,87	13,6%	16,2%
Castel San Pietro	**Bologna**	867	204,14	893	187,9	3,0%	8,0%

The main differences between the simulations and measurements are due to the manual driving, the eco-driving executed manually being not as precise as in the simulation model and the approximated execution of coast command. It was observed that consumption is measured during the “coast” periods. The manual driving introduces uncertainties in the estimation of energy consumption thus the estimation of energy savings associated to eco-driving are less precise than in trains equipped with ATO. During the entire journey between Rimini and Bologna, the eco-driving test reached energy savings of 38 % with respect to the reference case.

4.1.17 Sensitivity analysis on the energy saving determination

CMI, with the contribution of Comillas and ASTM, carried out a study of uncertainty propagation through the Train Simulator Algorithm (TSA). The algorithm is used to estimate train driving time, consumed and regenerated energy. These output quantities are important to optimise the driving profile of the train and minimise energy consumption. The uncertainty propagation was calculated using the Monte Carlo method. The sensitivity of output uncertainties on the input uncertainties was evaluated for two different train tracks in Spain, operated by Madrid Metro, and in Italy, between Bologna and Ozzano. The results described the sensitivity of the model and algorithm to the input parameters with respect to the saved energy.

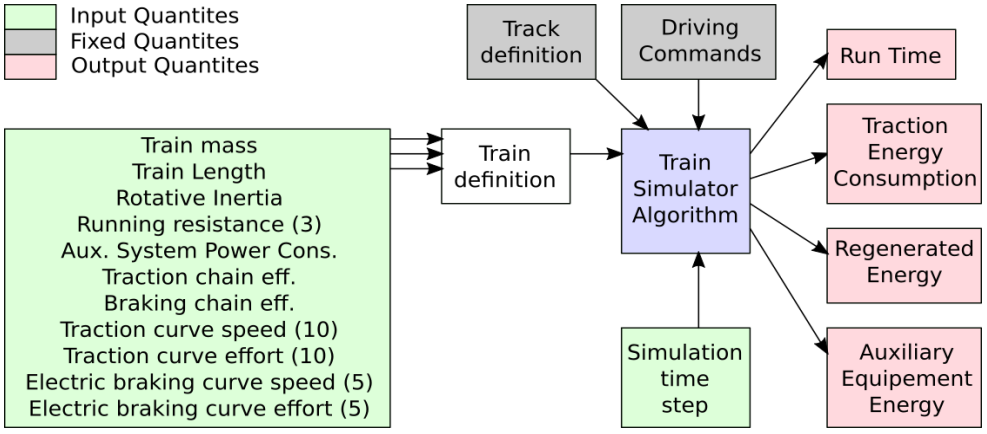

Figure 34 General outline of the TSA algorithm showing input, output and fixed (with zero uncertainty) quantities. The number in parenthesis shows number of matrix elements of the matrix input quantity.

Due to the its complex nature, the Monte Carlo method (JCGM, 2008) was implemented to evaluate the propagation of uncertainties through the TSA algorithm. The uncertainty was calculated for Bologna-Ozzano along the Bologna-Rimini track and line 10B of Metro de Madrid.

4.1.17.1 Sensitivity estimation

Two cases were considered for the sensitivity analysis. In the first case, all input uncertainties were set to zero and the uncertainty of one selected input quantity is varied from 10^{-14} to 10^{1}. In the second case, all the input quantities have an uncertainty of 5 % while the selected input quantity is varied between 1 % and 10 % This method was repeated for all input quantities. The results on the sensitivity are summarised in Figure 35 while the impact of the input uncertainty on the output quantity is provided for railway and metro study cases in Figure 36.

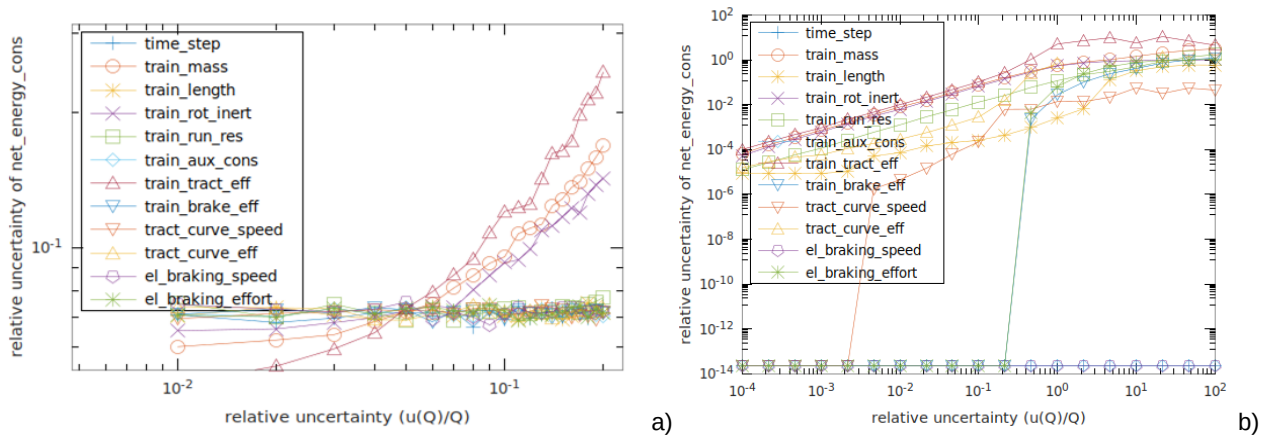

Figure 35 relative uncertainty of the consumed energy versus the relative uncertainty of the input quantities for the case 1 a) and case 2 b)

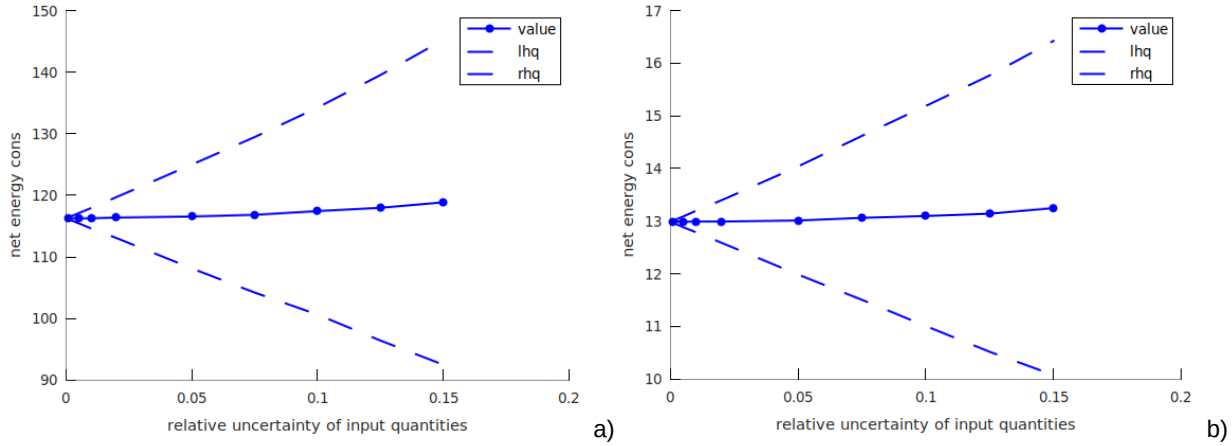

Figure 36 energy consumption versus the relative uncertainty of input quantities for railway case a) and metro case b). dashed lines indicate the upper and lower uncertainty limit.

4.1.18 Key output and conclusion

The collaboration among Comillas, ASTM, MM and CMI led to the development of the eco-driving algorithm and its application on line 10B of Metro de Madrid between Marqués de Valdavia y Hospital Infanta Sofía with four interstations with a class 9000 (length: 55 m, weight: 136 *t*, supplied in DC at 1500 V) rolling stock. For each interstation the test cases were characterised by the infrastructure information, the train information and the Automatic Train Operation system information (the on-board automatic driving equipment ATO). With this information the 4 interstations were modelled and simulated supposing initially a reference driving style (with the ATO), calculating the expected energy consumption and the running time. After that, an optimisation algorithm was executed to design the eco-driving, taking into account the specific characteristics of the ATO equipment on-board these trains running in line 10-B. Simulations provided an energy saving of about 33 % with a travel time increase of 26 seconds. The reliability of the simulations was proved by the measurement of the energy saving, that provides a saving of 33 % with an actual travel time of 22 seconds for the eco-driving journey.

Thanks to the measurements performed by INRIM and SUN with the support of Trenitalia and R.F.I., the eco-driving activity was performed on the DC railway line between Rimini and Bologna in Italy, with a test train used for regional connections with a weight of 361 Mg not equipped with ATO. The journey foresees 8 interstations; the line profile is characterised by a low plan-altimetry gradient. The eco-driving strategy, implemented manually was characterised by the following approach: to reach the maximum allowed speed then to nullify the traction effort, letting the train move by inertia, when the train lost too much speed, the traction effort was again increased in order to reach again the maximum speed. This approach provided energy savings of 38 %, corresponding to about 954 kWh with a travel time increase of 5 seconds. Merging the activity on the braking rheostat and on eco-driving, we can state that with a hypothetical efficient infrastructure able to

implement the eco-driving and the complete recovery of braking energy, energy savings of about 50 % can be reached on this journey.

A deep investigation on the sensitivity analysis of the uncertainty of the input quantities of the Train Simulation algorithm (TSA) was performed by CMI and Comillas with the contribution of ASTM. Due to the complexity of the model, a Monte Carlo approach was applied to estimate the combined uncertainty associated with run-time, the traction energy consumption, the regenerated energy and the auxiliary equipment energy.

In summary, The described project activities have provided means and methods to perform measurements of energy flow on-board trains with an accuracy lower than 1 %, thus meeting the project objective. The new methods have been applied to real test cases allowing a comparison between the eco-driving energy savings predicted by models and those estimated in-field. A detailed sensitivity analysis on the quantities affecting the estimated energy saving provided by the eco-driving has been carried out.

5 Impact

As of the end of the project, 42 articles were published in peer reviewed journals, 35 presentations of project activities were made at 17 international and 3 national conferences. In addition, the system developed during the project for the calibration of DC EMFs directly on-board was presented at a key Italian railway exhibition, the EXPO Ferroviaria. The project has also been promoted through various media outlets; 30 articles were published in the popular press, 3 press releases were issued, clips and videos were made available on RaiTV, YouTube, and dedicated pages were created on ResearchGate, Facebook and Youtube, which provide more information on the MyRailS. The dissemination has been supported by the production of 47 small videos describing not only the project activities but also the results and their importance for stakeholders.

The project webpage, found at http://myrails.it/, has drawn more than 170,000 visitors since July 2019. The Facebook page on MyRailS to which 47 videos and several posts have been uploaded has accumulated more than 1200 followers. The posts and videos have reached an audience of thousands.

Furthermore, the final workshop “Metrology and measurements for an efficient electric railway system,” devoted to the dissemination of the project results among the stakeholders and held in January 2021, met with considerable success. It was organised in collaboration with CIFI (Collegio degli Ingenegri Ferroviari Italiani), the Italian organisation for railway engineering. There were more than 250 registrations from many European countries as well as Japan and China. The workshop was broadcasted live on YouTube (https://www.youtube.com/watch?v=KAgsV1t-oFE); and more than 800 views were counted.

Impact on industrial and other user communities

New metrological services for the calibration of AC and DC EMF were established. The services allow the calibration of EMF both under pure AC and DC signals and in the presences of distortions for the AC and ripple for the DC. Testing of commercial DC and AC EMFs made available by stakeholders (HaslerRail and Mors Smitt) have been performed. These tests have been carried out by applying real voltage – current waveforms recorded in-field. The calibration system for railway EMFs is also of interest to manufacturers of combined voltage-current transducers for AC electric distribution grids, as well as to producers of smart terminations for MV cables that embed both voltage and current transducers. As their production has risen, new testing and calibration services capable of characterising these devices under real working conditions has become an emerging need.

The methods developed for the detection of arc events in DC railway systems will serve both infrastructure managers and railway companies. This tool deployed in conjunction with a widespread data collecting system could allow predictive maintenance of sliding contacts. In this framework, there is also considerable interest from manufacturers of EMFs drawn to the idea of embedding a new arc detection functionality in the EMF. With this, the number of arc events and their position in the railway network could be broadcasted by exploiting the ground data collection system already in use for energy billing. A database collecting the time-behaviour of the electric quantities at pantograph has been made freely available. Based on the experience gained through on-board measurements, the project has prepared a good practice guide for on-board energy flux estimation. The best practices defined in these guides will enable eco-driving energy saving assessments which will permit optimisation of ATO, improve the design of DC railway supply systems involving new RSS, and support better financial decision-making. It is worth noting that the participation of industrial partners in the project helped to align the project with industrial needs. The links now established between railway industry

partners and international and European railway consortia (UIC and CER) will guarantee notable uptake and exploitation of project output.

Impact on the metrological and scientific communities

The project outputs contributed to new calibration methods related to AC and DC compact electronic transducers supplied under actual harsh railway conditions. The information gathered will help the realisation of a harmonised calibration procedure, a reliable measurement model and a robust uncertainty budget. New/extended sensor calibration capabilities adapted to harsh non-sinusoidal conditions were developed and a guideline document for the whole energy meter chain calibration was made available to end users and the metrological community. The development of standard DC power for MV DC grids has triggered a process for the addition of DC power as a new quantity in the BIPM Key Comparison Database. In addition, the definition of PQ events and related metrics will have a significant scientific impact on the academic community dealing with the study of new LV and MV DC power transmission/distribution grids and relevant harmonic distortion.

Impact on relevant standards

The project consortium promoted the MyRailS results within the standardisation community and provided input to specific technical committees (CENELEC/IEC TC 9X, CENELEC/IEC TC 38 [WG 47 and WG 55]) on the subject of on-board energy measurements. The project was presented at the CEI CT 38 (the Italian standardisation technical committee on instrument transformers) during their periodic general assembly and at the annual meeting of the Sub-committee Power and Energy of the EURAMET TC-EM. Moreover, the project was introduced to IEC TC 9. The experience gathered through development of the calibration facilities for EMFs and the uncertainty budget estimation was made available to the maintenance group of the IEC 62888 standard “Energy measurement on board trains”. The coordinator, as an expert member of this technical committee, collected the contributions provided by some partners and proposed a new version of Annex C of IEC 62888-2 introducing a more rigorous metrological approach in estimation of the uncertainty associated with the power measurements performed by the AC EMFs. The proposal is under discussion. The project activities on reversible substations and monitoring of the voltage fluctuations were shared with IEC TC 9 and CENELEC TC 9X. As a consequence, the committees prepared a priority research topic, “Specifications for non-conventional DC substation and performance assessment of non-conventional subs,” which became the basis for the selected research topic (SRT), “Metrology support for enhanced energy efficiency in DC railway systems,” in the 2021 Normative call of the European Partnership on Metrology under Horizon Europe.

Longer-term economic, social and environmental impacts

At the outset of the project, it was the practice for many rail operators to charge for a train’s energy consumption based on a simple estimation. However, an error of 5 % on 36.5 TWh of energy used on European railways each year would equate to around 110M €. Accurate billing of energy consumption between rail network operators is essential for interoperability and is an important financial incentive. To that end, agreed and mutually accepted calibration tools, procedures and guidelines for the on-board energy measurement systems can increase mutual confidence in billing, fostering interoperability with reference to the rail ‘energy’ subsystem in the EU. To further improve energy efficiency, reliable tools for continuous monitoring of power quality events can be used to regulate energy billing, which will consider the electromagnetic impact of the user’s (the railway company’s) trains on the supply system and vice-versa.

In addition, it has been estimated that, for a single-track suburban line (30 km) with an annual traction consumption of 6 GWh, reversible substations can produce a saving of about 1.4 GWh (23 % of the traction consumption). The reduction of the energy dissipated by on-board braking rheostats will give a valuable contribution to solving the issue of tube temperature increase, which is detected by many underground network managers. A decrease of such temperature will consequently improve the energy efficiency of the traction units. Overall, by increasing the interoperability and integration of railway networks along with increased passenger confidence in the railway as a means of transport, the EU objectives of tripling the existing high-speed rail network by 2030 and moving the majority of medium distance passengers by rail by 2050 can be fulfilled.

In terms of environmental impact, train eco-driving techniques will improve PQ and can have a significant impact on the energy consumed for trains operating over the same route with the same stopping patterns. Coupled with the financial incentive enabled by a billing infrastructure, this should lead to significant energy saving and resultant reductions in emissions. By using accurate energy data and an optimised driving technique, the potential considering all the EU25 train drivers is estimated to be a yearly CO_2 emission reduction of 2.4 Mt. Moreover, the development of an integrated and energy efficient railway infrastructure at

European level, as fostered by the output of this project, will support the shift from medium distance road freight to rail freight green corridors.

Both social and environmental impact will be achieved, through widespread PQ monitoring system and data processing architecture which will prevent malfunctioning of railway electrical equipment thus ensuring greater confidence in the use of the electric public transport. This will also produce a reduction in car-use and have a positive impact on pollution-related health and environment problems, as well as, on the reduction of road congestion and the number of accidents, leading to an improvement in quality of life indexes.

6 List of publications

1. Delle Femine, D. Gallo, D. Giordano, C. Landi, M. Luiso, R. Visconte (2018), “A Set-up for Static and Dynamic Characterization of Voltage and Current Transducers used in Railway Application”, Journal of Physics: Conference Series, Volume 1065 052019, IOP Publishing, http://doi.org/10.1088/1742-6596/1065/5/052019
2. Delle Femine, D. Gallo, D. Giordano, C. Landi, M. Luiso, D. Signorino (2018), “Synchronized Measurement System for Railway Application”, XXII World Congress of the International Measurement Confederation (IMEKO 2018), Journal of Physics: Conference Series, Volume 1065 052040, http://doi.org/10.1088/1742-6596/1065/5/052040
3. G. Crotti, D. Giordano, A. Delle Femine, D. Gallo, C. Landi & M. Luiso (2018). “A Testbed for Static and Dynamic Characterization of DC Voltage and Current Transducers”, IEEE 9th International Workshop on Applied Measurements for Power Systems (AMPS), http://doi.org/10.5281/zenodo.3265102, https://doi.org/10.1109/AMPS.2018.8494873
4. D. Giordano, G. Crotti, P. Roccato, A. Delle Femine, D. Gallo, M. Luiso, A. Mariscotti (2019). "Pantograph-to-OHL Arc: Conducted Effects in DC Railway Supply System", IEEE Transactions on Instrumentation and Measurement, https://www.doi.org/10.1109/TIM.2019.2902805
5. Helko van den Brom, Ronald van Leeuwen, & Ralph Hornecker (2018). “Characterization of DC current sensors under distorted conditions for railway applications”, International Conference on Electrical Systems for Aircraft, Railway, Ship Propulsion and Road Vehicles (ESARS) and International Transportation Electrification Conference (ITEC) (ESARS-ITEC), http://doi.org/10.5281/zenodo.3265659, http://dx.doi.org/10.5281/zenodo.3265659
6. Helko van den Brom, Ronald van Leeuwen, & Ralph Hornecker (2019). “Characterization of DC Current Sensors with AC Distortion for Railway Applications”, IEEE Transactions on Instrumentation and Measurement, 68 (3), 2084–2090, https://zenodo.org/record/3265674#.XSyIEuhKhhF, http://dx.doi.org/10.1109/TIM.2019.2898014
7. G. Crotti, A. D. Femine, D. Gallo, D. Giordano, C. Landi and M. Luiso, "Calibration of Voltage and Current Transducers for DC Railway Systems," IEEE Transactions on Instrumentation and Measurement, 68 (2019), 3580-3860, http://doi.org/10.1109/TIM.2019.2912232
8. Delle Femine, Antonio, Gallo, Daniele, Landi, Carmine, & Luiso Mario. (2020), “Discussion on DC and AC Power Quality Assessment in Railway Traction Supply Systems,” 2019 International Instrumentation and Measurement Technology Conference (I2MTC), https://zenodo.org/record/3604218#.XhiVqUdKiCo;http://dx.doi.org/10.1109/I2MTC.2019.8826869
9. D. Signorino, G. Crotti, A. Delle Femine, D. Gallo, D. Giordano, C. Landi, M. Luiso, “Phantom Power Generator for DC Railway Metrology,” 2019 International Instrumentation and Measurement Technology Conference (I2MTC), https://doi.org/10.5281/zenodo.3597387
10. Mariscotti, D. Giordano, “Electrical Characteristics of Pantograph Arcs in DC Railways: Infrastructure Influence,” 24nd IMEKO TC4 International Symposium Electrical & Electronic Measurements, http://doi.org/10.5281/zenodo.3604345, https://www.imeko.org/publications/tc42019/IMEKO-TC4-2019-033.pdf
11. Mariscotti, Andrea, “Discussion of Power Quality Metrics suitable for DC Power Distribution and Smart Grids“, 24nd IMEKO TC4 International Symposium Electrical & Electronic Measurements, http://doi.org/10.5281/zenodo.3604343

12. Mariscotti, Andrea, “Relevance of Harmonic Active Power Terms for Energy Consumption in Some Railway Systems (Version 05),” 24nd IMEKO TC4 International Symposium Electrical & Electronic Measurements, http://doi.org/10.5281/zenodo.3604338,https://www.imeko.org/publications/tc4-2019/IMEKO-TC4-2019-026.pdf
13. Delle Femine, D. Gallo, D. Giordano, C. Landi, M.Luiso, D. Signorino, “Power Quality Assessment in Railway Traction Supply Systems,“ IEEE Transactions on Instrumentation and Measurement, 69 (2020), 2355-2366, http://dx.doi.org/10.1109/TIM.2020.2967162
14. G. Crotti; D. Giordano; D. Signorino; A. Delle Femine; D. Gallo; C. Landi; M. Luiso; A. Biancucci; L. Donadio, “Monitoring Energy and Power Quality On Board Train,“ Proc. 2019 IEEE 10th International Workshop on Applied Measurements for Power Systems (AMPS), https://zenodo.org/record/4598462#.YGDLt2gzaCo
15. Y. Seferi, P. Clarkson, S. M. Blair, A. Mariscotti and B. G. Stewart, “Power Quality Event Analysis in 25 kV 50 Hz AC Railway System Networks,“ Proc. 2019 IEEE 10th International Workshop on Applied Measurements for Power Systems (AMPS), http://dx.doi.org/10.1109/AMPS.2019.8897765
16. Mariscotti, D. Giordano, A. D. Femine and D. Signorino, "Filter Transients onboard DC Rolling Stock and Exploitation for the Estimate of the Line Impedance," 2020 IEEE International Instrumentation and Measurement Technology Conference (I2MTC), Dubrovnik, Croatia, 2020, pp. 1-6, http://doi.org/10.1109/I2MTC43012.2020.9128903
17. G. Cipolletta et al., "Monitoring a DC Train Supplied by a Reversible Substation," 2020 IEEE International Instrumentation and Measurement Technology Conference (I2MTC), Dubrovnik, Croatia, 2020, pp. 1-6, http://doi.org/10.1109/I2MTC43012.2020.9128644
18. F. Cascetta, G. Cipolletta, A. Delle Femine, D. Gallo, D. Giordano, D. Signorino, “Measuring the impact of reversible substations on energy efficiency in rail transport,” Proc. 24th IMEKO TC4 International Symposium, https://www.imeko.org/publications/tc4-2020/IMEKO-TC4-2020-24.pdf
19. Giordano Domenico, Signorino Davide, Landi Carmine, Delle Femine Antonio, Luiso Mario, Crotti Gabriella, “Power quality in DC railway system: A facility to characterize the on-board detection systems,” Proc. 24th IMEKO TC4 International Symposium, http://doi.org/10.5281/zenodo.4589149
20. H. van den Brom, D. Giordano, D. Gallo, A. Wank and Y. Seferi, "Accurate Measurement of Energy Dissipated in Braking Rheostats in DC Railway Systems," 2020 Conference on Precision Electromagnetic Measurements (CPEM), Denver, CO, USA, 2020, pp. 1-2, http://doi.org/10.1109/CPEM49742.2020.9191917
21. H. van den Brom and R. van Leeuwen, "Calibrating Sensors to Measure Braking Chopper Currents in DC Traction Units," 2020 Conference on Precision Electromagnetic Measurements (CPEM), Denver, CO, USA, 2020, pp. 1-2, http://doi.org/10.1109/CPEM49742.2020.9191822
22. R. van Leeuwen, H. van den Brom, G. Rietveld, E. Houtzager and D. Hoogenboom, "Measuring the Voltage Dependence of Current Transformers," 2020 Conference on Precision Electromagnetic Measurements (CPEM), Denver, CO, USA, 2020, pp. 1-2, http://doi.org/10.1109/CPEM49742.2020.9191845
23. G. Crotti et al., "Calibration System for DC Power/Energy Measurement chain in Railway applications," 2020 Conference on Precision Electromagnetic Measurements (CPEM), Denver, CO, USA, 2020, pp. 1-2, http://doi.org/10.1109/CPEM49742.2020.9191718
24. Mariscotti, D. Giordano, A. D. Femine, D. Gallo and D. Signorino, "How Pantograph Electric Arcs affect Energy Efficiency in DC Railway Vehicles," 2020 IEEE Vehicle Power and Propulsion Conference (VPPC), Gijon, Spain, 2020, pp. 1-5, http://doi.org/10.1109/VPPC49601.2020.9330954
25. Jorge Rovira. “Calibration set-up for energy measuring systems installed in AC railway systems,” Proc. 2020 IEEE Vehicle Power and Propulsion Conference (VPPC), http://doi.org/10.5281/zenodo.4588726
26. F. Fan and B. G. Stewart, "Power Flow Simulation of DC Railway Power Supply Systems with Regenerative Braking," 2020 IEEE 20th Mediterranean Electrotechnical Conference (MELECON), Palermo, Italy, 2020, pp. 87-92, http://doi.org/10.1109/MELECON48756.2020.9140462

27. F. Fan, A. Wank, Y. Seferi and B. G. Stewart, "Pantograph Arc Location Estimation using Resonant Frequencies in DC Railway Power Systems," IEEE Transactions on Transportation Electrification, 2021, http://doi.org/10.1109/TTE.2021.3062229
28. Andrea Mariscotti, “Uncertainty of the Energy Measurement Function deriving from Distortion Power Terms for a 16.7 Hz Railway,” Acta IMEKO, vol. 9, no. 2, article 5, June 2020, http://dx.doi.org/10.21014/acta_imeko.v9i2.764
29. Istrate, D., Khamlichi, A., Soccalingame, S., Rovira, J., Fortune, D., Sira, M., Simon, P., Garnacho, F., “Laboratory Calibration of Energy Measurement Systems (EMS) under AC Distorted Waveforms,” Sensors 2020, 20, 6301. https://doi.org/10.3390/s20216301
30. Giordano, D., Signorino, D., Gallo, D., van den Brom, H.E., Sira, M., “Methodology for the Accurate Measurement of the Power Dissipated by Braking Rheostats,” Sensors 2020, 20, 6935. https://doi.org/10.3390/s20236935
31. Andrea Mariscotti, Domenico Giordano, “Experimental Characterization of Pantograph Arcs and Transient Conducted Phenomena in DC Railways,” Acta IMEKO, vol. 9, no. 2, article 3, June 2020, identifier: IMEKO-ACTA-09 (2020)-02-03. http://dx.doi.org/10.21014/acta_imeko.v9i2.761
32. Seferi, Y., Blair, S.M., Mester, C., Stewart, B.G., “Power Quality Measurement and Active Harmonic Power in 25 kV 50 Hz AC Railway Systems,” Energies 2020, 13, 5698, https://doi.org/10.3390/en13215698
33. Seferi, Y., Blair, S.M., Mester, C., Stewart, B.G., “A Novel Arc Detection Method for DC Railway Systems,” Energies 2021, 14, 444, https://doi.org/10.3390/en14020444
34. Davide Signorino, Domenico Giordano, Andrea Mariscotti, Daniele Gallo, Antonio Delle Femine, Fabio Balic, Jorge Quintana, Lorenzo Donadio, Alfredo Biancucci, “Dataset of measured and commented pantograph electric arcs in DC railways,” Data in Brief, 31, 2020, 105978, ISSN 2352-3409, https://doi.org/10.1016/j.dib.2020.105978.
35. D. Istrate, D. Fortuné, “Fictive power source for calibrations in railway systems,” 19th International Congress of Metrology (CIM2019), 1 (2019), 08001, https://doi.org/10.1051/metrology/201908001
36. D. Giordano, G. Crotti, D. Gallo, M. Luiso, A. Delle Femine, N. Filippini, I. Rossetta, C. Splavieri, L. Donadio, A. Mariscotti, “Pantograph-Catenary Arc Detection Technique based on Conducted Effects Measurement on Railway Supply System,” WCCR Papers, 2019, https://doi.org/10.5281/zenodo.4587794
37. F. Garnacho, J. Rovira, A. Khamlichi, P. Simón, I. Garrido, “Reference Energy Measuring System for On-Board Calibration of EMS Installed in Locomotives,” International Conference on Sensors Engineering and Electronics Instrumentation Advances (SEIA), September 2020, Porto, Portugal, http://dx.doi.org/10.5281/zenodo.4588736
38. Andrea Mariscotti, “Experimental characterisation of active and non-active harmonic power flow of AC rolling stock and interaction with the supply network,” IET Electrical Systems in Transportation 1, 2021, https://doi.org/10.1049/els2.12009
39. Mariscotti, A., “Characterization of Active Power Flow at Harmonics for AC and DC Railway Vehicles,” 2019 IEEE Vehicle Power and Propulsion Conference (VPPC) 1, 6, http://dx.doi.org/10.1109/VPPC46532.2019.8952310
40. Mariscotti, A., “Behaviour of Spectral Active Power Terms for the Swiss 15 kV 16.7 Hz Railway System,” 2019 IEEE 10th International Workshop on Applied Measurements for Power Systems (AMPS), http://dx.doi.org/10.1109/AMPS.2019.8897777

This list is also available here: https://www.euramet.org/repository/research-publications-repository-link/